

WAVES ON ACCELERATING DODECAHEDRAL UNIVERSES

A. BACHELOT-MOTET AND A. BACHELOT

ABSTRACT. We investigate the wave propagation on a compact 3-manifold of constant positive curvature with a non trivial topology, the Poincaré dodecahedral space, when the scale factor is exponentially increasing. We prove the existence of a limit state as $t \rightarrow +\infty$ and we get its analytic expression. We transform the Cauchy problem into a mixed problem posed on a fundamental domain determined by the quaternionic calculus. We perform an accurate scheme of computation: we employ a variational method using a space of second order finite elements that is invariant under the action of the binary icosahedral group.

I. INTRODUCTION

The topology and the geometry of our universe is a fundamental open problem. There are a lot of articles about these topics (for example [15, 16, 25]). Recently the data by WMAP (Wilkinson Microwave Anisotropy Probe) mission have provided strong evidence suggesting that the observable universe is nearly flat, with the ratio of its total matter-energy density to the critical value very close to one [4], but without fixing the sign of its curvature. So the study of the wave propagation in universes involving the Poincaré dodecahedral space continues to be relevant. This model has received a lot of interest and generated numerous works (see *e.g.* [1, 3, 5, 12, 17, 20, 26]). These spacetimes are Lorentzian manifolds $(\mathbb{R}_t \times \mathbf{K}, g)$ that are globally hyperbolic and multi-connected. Here \mathbf{K} is the Poincaré dodecahedral space that is a three dimensional C^∞ compact manifold, without boundary, defined as the quotient of the 3-sphere \mathcal{S}^3 under the action of the binary icosahedral group \mathcal{I}^* ([8, 21, 24, 27]). In [3] we have investigated the propagation of the scalar waves in the case of the stationary universe for which $ds^2 = dt^2 - ds_{\mathbf{K}}^2$ where $ds_{\mathbf{K}}^2$ is the Euclidean metric induced by the three-sphere \mathcal{S}^3 on \mathbf{K} . In this paper we study the wave propagation on dynamical universes (\mathcal{U}, g) of Robertson-Walker type

$$(I.1) \quad \mathcal{U} = \mathbb{R}_t \times \mathbf{K}, \quad ds_{\mathcal{U}}^2 = g_{\mu\nu} dx^\mu dx^\nu = dt^2 - a^2(t) ds_{\mathbf{K}}^2,$$

where the scale factor $a(t)$ is a smooth positive function. We are mainly interested in considering the accelerating spacetimes for which the scale factor is an increasing function with an exponential behaviour, $a(t) \sim e^{\alpha t}$ as $t \rightarrow \infty$. In the study of the asymptotics of the fields at the infinity, and for the numerical experiments, we treat two important cases. In the first one, we choose $a(t) = H^{-1} \cosh(Ht)$ where $H > 0$ is the Hubble constant. Then g is solution of the vacuum Einstein equations with cosmological constant $\Lambda = 3H^2$ and \mathcal{U} is locally isometric to the De Sitter spacetime $d\mathcal{S}_4$ and differs globally from $d\mathcal{S}_4$ by its topology that is not trivial. We denote this universe $d\mathcal{S}_4(\mathbf{K})$. In particular, while $d\mathcal{S}_4$ is spatially homogeneous and globally isotropic, $d\mathcal{S}_4(\mathbf{K})$ is homogeneous but not globally isotropic [18]. In the second model we choose $a(t) = e^t$. Then g is no longer a solution of the vacuum Einstein equations but it is a toy model for a universe with an inflation generated by a scalar field or a solution in $f(T)$ theory (see *e.g.* [9]).

In this paper we investigate the scalar waves on (\mathcal{U}, g) that are the solutions of the D'Alembert equation

$$\square_g \Psi := \frac{1}{\sqrt{|g|}} \partial_\mu \left(g^{\mu\nu} \sqrt{|g|} \partial_\nu \Psi \right) = 0.$$

For the spacetime (I.1), this equation has the form

$$(I.2) \quad \left[\partial_t^2 + 3 \frac{a'(t)}{a(t)} \partial_t - \frac{1}{a^2(t)} \Delta_{\mathbf{K}} \right] \Psi = 0, \quad t \in \mathbb{R}, \quad x \in \mathbf{K},$$

where $\Delta_{\mathbf{K}}$ is the Laplace-Beltrami operator on \mathbf{K} . In part 2 we solve the global Cauchy problem for (I.2) in the functional framework associated to the energy

$$(I.3) \quad E(\Psi, t) := \|\partial_t \Psi(t)\|_{L^2(\mathbf{K})}^2 + \frac{1}{a^2(t)} \|\nabla_{\mathbf{K}} \Psi(t)\|_{L^2(\mathbf{K})}^2.$$

We represent the Poincaré dodecahedral space by its fundamental domain \mathcal{F} that is the geodesic convex hull of twenty vertices on \mathcal{S}^3 that are included in $\{x_0 = \frac{\sigma^2}{2\sqrt{2}}\} \times \mathbb{R}^3$ where σ is the golden ratio. We introduce the domain of visualisation $\mathcal{F}_v \subset \mathbb{R}^3$ that is the projection $(x_0, x_1, x_2, x_3) \in \mathcal{S}^3 \mapsto (x_1, x_2, x_3) \in \mathbb{R}^3$ of the fundamental domain. \mathcal{F}_v is a dodecahedron with pentagonal curved faces included in ellipsoids (figure 1). Defining $u(t, x_1, x_2, x_3) := \Psi(t, x_0, x_1, x_2, x_3)$ the wave equation (I.2) is equivalent to

$$(I.4) \quad \left[\partial_t^2 + 3 \frac{a'(t)}{a(t)} \partial_t - \frac{1}{a^2(t)} \Delta_{\mathcal{F}_v} \right] u = 0, \quad t \in \mathbb{R}, \quad x \in \mathcal{F}_v,$$

together with the boundaries conditions

$$(I.5) \quad \forall \tau \in \mathcal{I}^*, (x'_0, x'_1, x'_2, x'_3) = \tau(x_0, x_1, x_2, x_3) \Rightarrow u(t, x'_1, x'_2, x'_3) = u(t, x_1, x_2, x_3).$$

In the third section we investigate the asymptotic behaviour of $\Psi(t, \cdot)$ as $t \rightarrow +\infty$. We prove the existence of an asymptotic profile $\Psi_\infty := \lim_{t \rightarrow \infty} \Psi(t)$ when the scale factor is exponentially increasing, and we compute an analytic expression of Ψ_∞ in the cases $a(t) = H^{-1} \cosh(Ht)$ and $a(t) = e^t$. These results extend those of [2] for the steady state universe (see also [23]). In the fourth part we numerically investigate the mixed problem (I.4, I.5). We are mainly interested in computing the waves for a long time, hence the exponential behaviour of the coefficients in the equation leads to a hard numerical challenge. To overcome this difficulty we have to perform very precise computations. To reach this goal we adopt the variational method associated to (I.4) with suitable finite elements satisfying constraint (I.5). In the case of the stationary universes we have used in [3] finite elements of \mathbb{P}_1 type. To be able to treat the accelerating universes, we need more precision and we use elements of second order. Our numerical results are in excellent agreement with the theoretical results on the asymptotic behaviours of the waves.

II. WAVES ON DYNAMICAL UNIVERSES

In this section we solve the global Cauchy problem for the D'Alembert equation on the dynamical universes (I.1). We assume the scale factor a is a C^∞ function that is strictly positive. Then we know that (\mathcal{U}, g) is a globally hyperbolic manifold and according to Leray [14] the global Cauchy problem is well posed in C^∞ . Now it is natural to look for the solutions in the scale of the Hilbert spaces associated to the energy (I.3). Given $m \in \mathbb{N}$, we introduce the Sobolev space

$$H^m(\mathbf{K}) := \{ \Psi \in L^2(\mathbf{K}), \nabla_{\mathbf{K}}^\alpha \Psi \in L^2(\mathbf{K}), |\alpha| \leq m \}.$$

where $\nabla_{\mathbf{K}}$ are the covariant derivatives. We can also interpret this space as the set of the distributions Ψ that belong to the usual Sobolev space $H^m(\mathcal{S}^3)$ such that $\Psi \circ \tau = \Psi$ for any $\tau \in \mathcal{I}^*$. We use also the space $H^{-1}(\mathbf{K})$ that is the dual space of $H^1(\mathbf{K})$.

Theorem II.1. *Given $m \in \mathbb{N}$, $\Psi_0 \in H^{m+1}(\mathbf{K})$, $\Psi_1 \in H^m(\mathbf{K})$, $t^* \in \mathbb{R}$, there exists a unique solution Ψ of the wave equation (I.2) satisfying*

$$(II.1) \quad \Psi \in C^0(\mathbb{R}_t; H^{m+1}(\mathbf{K})) \cap C^1(\mathbb{R}_t; H^m(\mathbf{K})),$$

$$(II.2) \quad \Psi(t^*, \cdot) = \Psi_0(\cdot), \quad \partial_t \Psi(t^*, \cdot) = \Psi_1(\cdot).$$

For $m = 0$, Ψ is the unique solution satisfying together (II.1), (II.2), and for all $\Phi \in H^1(\mathbf{K})$

$$(II.3) \quad \frac{d^2}{dt^2} \langle \Psi(t), \Phi \rangle_{L^2(\mathbf{K})} + 3 \frac{a'(t)}{a(t)} \frac{d}{dt} \langle \Psi(t), \Phi \rangle_{L^2(\mathbf{K})} + \frac{1}{a^2(t)} \langle \nabla_{\mathbf{K}} \Psi(t), \nabla_{\mathbf{K}} \Phi \rangle_{L^2(\mathbf{K})} = 0.$$

When the scale factor $a(t)$ is increasing then the energy defined by (I.3) is decreasing.

Remark When $m = 0$, Ψ is called “finite energy solution”. Since Ψ is a solution of (I.2), we remark that Ψ belongs to $C^2(\mathbb{R}_t; H^{-1}(\mathbf{K}))$. Therefore $\langle \Psi(t), \Phi \rangle_{H^{-1}(\mathbf{K}), H^1(\mathbf{K})} = \langle \Psi(t), \Phi \rangle_{L^2(\mathbf{K})} \in C^2(\mathbb{R}_t)$ and the first term in (II.3) is well defined. When $\Psi_j \in C^\infty(\mathbf{K})$, then $\Psi \in C^\infty(\mathbb{R}_t \times \mathbf{K})$, and we say that Ψ is a “smooth solution”.

Proof. There are a lot of ways to obtain the theorem from well known results. To construct the solutions we could invoke the existence of the smooth solutions by the theorem of Leray [14], then we extend by density of C^∞ in $H^m(\mathbf{K})$ by using the energy estimate satisfied by the regular solutions:

$$(II.4) \quad \frac{d}{dt} E(\Psi, t) = -6 \frac{a'(t)}{a(t)} \|\partial_t \Psi(t)\|_{L^2(\mathbf{K})}^2 - 2 \frac{a'(t)}{a^3(t)} \|\nabla_{\mathbf{K}} \Psi(t)\|_{L^2(\mathbf{K})}^2.$$

Then by the Grönwall lemma we can control the energy at any time, hence we get the global solutions for $m = 0$. Finally commuting the covariant derivatives and the D'Alembert operator, we deduce the existence of solutions for any $m \in \mathbb{N}$. Another way consists in employing the spectral method of Kato (see *e.g.* [22]). In fact the more convenient approach to directly obtain the existence, the uniqueness and the equivalence with the variational problem is the variational method by Lions. We can easily see that our Theorem is a direct application of the results of chapter XVIII of [7].

□

To perform a computational method to solve the Cauchy problem, it is convenient to represent the Poincaré dodecahedron \mathbf{K} by a solid \mathcal{F}_v in \mathbb{R}^3 . We recall that \mathbf{K} is the quotient of the 3-sphere \mathcal{S}^3 under the action of the discrete fixed-point free subgroup \mathcal{I}^* of isometries of \mathcal{S}^3 , with \mathcal{I}^* acting by left multiplication (see [1, 3, 5, 12, 17, 20]). The subgroup \mathcal{I}^* of $SO(4)$ is the binary icosahedral group ([8, 21, 24, 27]). It is a two sheeted covering of the icosahedral group $\mathcal{I} \subset SO(3)$ consisting of all orientation-preserving symmetries of a regular icosahedron.

To construct \mathcal{F}_v , we represent $\mathcal{S}^3/\mathcal{I}^*$ by a fundamental domain $\mathcal{F} \subset \mathcal{S}^3$ and an equivalence relation \sim such that

$$(II.5) \quad \mathcal{S}^3/\mathcal{I}^* = \mathcal{F}/\sim.$$

The construction is based on the quaternionic calculus. It is detailed in [3]. Here we just present the main features. \mathcal{F} is such that:

$$(II.6) \quad \mathcal{S}^3 = \bigcup_{\tau \in \mathcal{I}^*} \tau(\mathcal{F}), \quad \text{and} \quad \forall \tau \in \mathcal{I}^*, \forall \tau' \in \mathcal{I}^*, \tau \neq \tau' \Rightarrow \tau \left(\overset{\circ}{\mathcal{F}} \right) \cap \tau' \left(\overset{\circ}{\mathcal{F}} \right) = \emptyset.$$

\mathcal{F} is a regular spherical dodecahedron (dual of a regular icosahedron). One hundred twenty such spherical dodecahedra tile the 3-sphere in the pattern of a regular 120-cell. More specifically we choose the fundamental domain such that $(1, 0, 0, 0) \in \mathcal{F}$, then \mathcal{F} is the geodesic convex hull in \mathcal{S}^3 of these 20 vertices: $\frac{1}{2\sqrt{2}}(\sigma^2, \pm\frac{1}{\sigma^2}, 0, \pm 1)$, $\frac{1}{2\sqrt{2}}(\sigma^2, 0, \pm 1, \pm\frac{1}{\sigma^2})$, $\frac{1}{2\sqrt{2}}(\sigma^2, \pm\frac{1}{\sigma}, \pm\frac{1}{\sigma}, \pm\frac{1}{\sigma})$ and $\frac{1}{2\sqrt{2}}(\sigma^2, \pm 1, \pm\frac{1}{\sigma^2}, 0)$, where $\sigma = (1 + \sqrt{5})/2$ is the golden number. Each of the 12 faces of \mathcal{F} is a regular pentagon in \mathcal{S}^3 (see [3], for details).

The equivalence relation \sim is defined by specifying the equivalence class \dot{q} of $q \in \mathcal{F}$. It is built from twelve Clifford translations g_i that have been used for the construction of \mathcal{F} (see Appendix A and [3]):

$$\dot{q} = \left\{ g_i(q), i \in \{1, \dots, 12\} \right\} \cap \mathcal{F}.$$

It follows that: (1) if q belongs to $\overset{\circ}{\mathcal{F}}$, then \dot{q} has only one element, (2) if q is a vertex of \mathcal{F} , then \dot{q} has four elements, (3) if q belongs to an edge of a face, without being a vertex, then \dot{q} has three elements, (4) if q belongs to a face and does not belong to an edge, then \dot{q} has two elements.

Finally to define \mathcal{F}_v we use the projection $p : (x_0, x_1, x_2, x_3) \in \mathcal{S}^3 \mapsto (x_1, x_2, x_3) \in \mathbb{R}^3$, and we choose $\mathcal{F}_v := p(\mathcal{F})$. With our choice of fundamental domain p is one-to-one on \mathcal{F} and we have

$$(II.7) \quad (x, y, z) \in \mathcal{F}_v \iff (\sqrt{1 - x^2 - y^2 - z^2}, x, y, z) \in \mathcal{F}.$$

The vertices of \mathcal{F}_v are those of a centered regular dodecahedron in \mathbb{R}^3 and they are given by $\frac{1}{2\sqrt{2}}(\pm\frac{1}{\sigma^2}, 0, \pm 1)$, $\frac{1}{2\sqrt{2}}(0, \pm 1, \pm\frac{1}{\sigma^2})$, $\frac{1}{2\sqrt{2}}(\pm\frac{1}{\sigma}, \pm\frac{1}{\sigma}, \pm\frac{1}{\sigma})$ and $\frac{1}{2\sqrt{2}}(\pm 1, \pm\frac{1}{\sigma^2}, 0)$. Each face of \mathcal{F}_v is included in an ellipsoid [3]. The equivalence relation \sim on \mathcal{F} induces canonically an equivalence relation \sim on \mathcal{F}_v :

$$(II.8) \quad \forall X, X' \in \mathcal{F}, X \sim X' \iff p(X) \sim p(X').$$

\sim leaves invariant the interior of \mathcal{F}_v and identifies any pentagonal face of \mathcal{F}_v with its opposite face, after rotating by $\frac{\pi}{5}$ clockwise around the outgoing normal at the center of this last face.

Obviously Ψ is entirely determined on $\mathbb{R}_t \times \mathbf{K}$ by its restriction to $\mathbb{R}_t \times \mathcal{F}$, hence we are going to work on $\mathbb{R}_t \times \mathcal{F}_v$. We introduce the map $f : (x, y, z) \in \mathcal{F}_v \mapsto f(x, y, z) = (\sqrt{1 - x^2 - y^2 - z^2}, x, y, z) \in \mathcal{S}^3$. f is one-to-one from $\mathcal{F}_v \subset \mathbb{R}^3$ onto $\mathcal{F} \subset \mathcal{S}^3$ and we put

$$(II.9) \quad u(t, x, y, z) := \Psi(t, f(x, y, z)).$$

It is clear that $\Phi \in H^1(\mathbf{K})$ iff $v := \Phi \circ f$ belongs to the usual Sobolev space H^1 on \mathcal{F}_v for the euclidean metric of \mathbb{R}^3 , $H^1(\mathcal{F}_v) = \{v \in L^2(\mathcal{F}_v), \nabla_{x,y,z} v \in L^2(\mathcal{F}_v)\}$, and satisfies the boundary condition

$$\forall X, X' \in \partial\mathcal{F}_v, X \sim X' \Rightarrow v(X) = v(X').$$

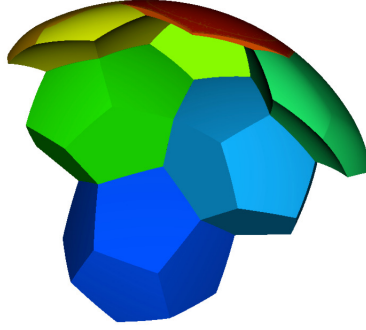


FIGURE 1. The Fundamental Domain (dark blue). We display \mathcal{F}_v (in dark blue) and the projection p in \mathbb{R}^3 of the images of \mathcal{F} by six elements of \mathcal{I}^* . It is the representation of a part of the tiling of \mathcal{S}^3 .

We deduce that $\Psi \in C^0(\mathbb{R}_t; H^1(\mathbf{K})) \cap C^1(\mathbb{R}_t; L^2(\mathbf{K}))$ is solution of (I.2) iff u belongs to $C^0(\mathbb{R}_t; H^1(\mathcal{F}_v)) \cap C^1(\mathbb{R}_t; L^2(\mathcal{F}_v))$ and satisfies the equation (I.4) where

$$(II.10) \quad \Delta_{\mathcal{F}_v} = (1-x^2)\partial_{11}^2 + (1-y^2)\partial_{22}^2 + (1-z^2)\partial_{33}^2 - 2xy\partial_{12}^2 - 2xz\partial_{13}^2 - 2yz\partial_{23}^2 - 3x\partial_1 - 3y\partial_2 - 3z\partial_3,$$

and the boundary conditions

$$(II.11) \quad \forall (t, X, X') \in \mathbb{R} \times \partial\mathcal{F}_v \times \partial\mathcal{F}_v, \quad X \sim X' \Rightarrow u(t, X) = u(t, X').$$

To handle the boundary when applying the finite element method, it is very convenient to take into account the boundary condition (II.11) by a suitable choice of the functional space. In the sequel we denote $X := (x, y, z)$, $|X|^2 := x^2 + y^2 + z^2$ and $dX := dx dy dz$. For $m = -1, 0, 1$, we introduce the spaces $W^m(\mathcal{F}_v)$ that are isometric to the spaces $H^m(\mathbf{K})$:

$$(II.12) \quad W^0(\mathcal{F}_v) := L^2(\mathcal{F}_v, (1-|X|^2)^{-\frac{1}{2}}dX),$$

$$(II.13) \quad W^1(\mathcal{F}_v) := \{u \in H^1(\mathcal{F}_v), \quad X \sim X' \Rightarrow u(X) = u(X')\}, \quad \|u\|_{W^1}^2 := \sum_{|\alpha| \leq 1} \|\partial^\alpha u\|_{W^0(\mathcal{F}_v)}^2,$$

$$(II.14) \quad W^{-1}(\mathcal{F}_v) := (W^1(\mathcal{F}_v))' = \{\Phi \circ f, \quad \Phi \in H^{-1}(\mathbf{K})\}.$$

We have $u \in C^k(\mathbb{R}_t, W^m(\mathcal{F}_v))$ iff $\Psi \in C^k(\mathbb{R}_t; H^m(\mathbf{K}))$ and Theorem II.1 can be expressed in terms of u as the following

Theorem II.2. *Given $u_0 \in W^1(\mathcal{F}_v)$, $u_1 \in W^0(\mathcal{F}_v)$, $t^* \in \mathbb{R}$, there exists a unique u solution of the equation (I.4) and satisfying*

$$(II.15) \quad u \in C^0(\mathbb{R}_t^+; W^1(\mathcal{F}_v)) \cap C^1(\mathbb{R}_t^+; W^0(\mathcal{F}_v)) \cap C^2(\mathbb{R}_t^+; W^{-1}(\mathcal{F}_v)),$$

$$(II.16) \quad u(t^*, \cdot) = u_0(\cdot), \quad \partial_t u(t^*, \cdot) = u_1(\cdot).$$

u is the unique function satisfying (II.15), (II.16) and such that for any $\phi \in W^1(\mathcal{F}_v)$, we have:

$$0 = \frac{d^2}{dt^2} \int_{\mathcal{F}_v} (1 - |X|^2)^{-\frac{1}{2}} u(t, X) \phi(X) dX + 3 \frac{a'(t)}{a(t)} \frac{d}{dt} \int_{\mathcal{F}_v} (1 - |X|^2)^{-\frac{1}{2}} u(t, X) \phi(X) dX \\ + \frac{1}{a^2(t)} \int_{\mathcal{F}_v} (1 - |X|^2)^{-\frac{1}{2}} [\nabla_X u(t, X) \cdot \nabla_X \phi(X) - (X \cdot \nabla_X u(t, X)) (X \cdot \nabla_X \phi(X))] dX.$$

We end this part by discussing the possible horizons in the dynamical universe (I.1). We recall that the comoving spatial distance d between any two points x and y on \mathcal{S}^3 is given by: $d(x, y) = \arccos[x^i y_j]$. \mathcal{F}_v is endowed with the distance induced by d . Moreover the largest distance d_{max} between the origin and the boundary of \mathcal{F}_v is reached at any of its vertices. So we have $d_{max} = \arccos\left(\frac{\sigma^2}{2\sqrt{2}}\right) \simeq 0.388$. The metric on $\mathbb{R}_t \times \mathcal{F}_v$ can be expressed in spherical coordinates $\rho = |X|$, $\omega = \rho^{-1}X$, by $ds^2 = dt^2 - a^2(t) \left(\frac{1}{1-\rho^2} d\rho^2 + \rho^2 d\omega^2\right)$ where $\omega \in \mathcal{S}^2$, $0 \leq \rho \leq \rho_{max}(\omega)$. We have $R_{max} := \sup_{\omega \in \mathcal{S}^2} \rho_{max}(\omega) = \sin(d_{max}) = \sqrt{1 - \frac{\sigma^4}{8}} \simeq 0.378$. Given $t^* \in \mathbb{R}$, $0 \leq R < R_{max}$ we investigate the future causal domain $\mathcal{O}^+(t^*, R)$ of $\{t^*\} \times (\mathcal{F}_v \cap ([0 \leq \rho \leq R] \times \mathcal{S}^2))$. Solving

$$(II.17) \quad \frac{\rho'(t)}{\sqrt{1 - \rho^2(t)}} = \frac{1}{a(t)},$$

we get that

$$\mathcal{O}^+(t^*, R) = \bigcup_{t \geq t^*} \{t\} \times (\mathcal{F}_v \cap ([0 \leq \rho \leq R(t)] \times \mathcal{S}^2))$$

where

$$(II.18) \quad R(t) = \sin \left(\arcsin(R) + \int_{t^*}^t \frac{1}{a(s)} ds \right)$$

provided that $\arcsin(R) + \int_{t^*}^t \frac{1}{a(s)} ds \leq \pi/2$. Therefore an interesting phenomenon appears when

$$(II.19) \quad \arcsin(R) + \int_{t^*}^{\infty} \frac{1}{a(s)} ds < \arcsin(R_{max}) = d_{max}.$$

In this case, a horizon exists:

$$(II.20) \quad \mathcal{O}^+(t^*, R) \subset [t^*, \infty) \times [0, R_h] \times \mathcal{S}^2,$$

where the radius of this horizon is

$$(II.21) \quad R_h := \sin \left(\arcsin(R) + \int_{t^*}^{\infty} \frac{1}{a(s)} ds \right).$$

Returning to the scalar waves, we conclude that if u_0 and u_1 are supported in $\rho \leq R$, then for any $t \geq t^*$, $u(t)$ is supported in $\rho \leq R_h$. Finally we give the expression of these quantities for the two accelerating universes that we consider $d\mathcal{S}_4(\mathbf{K})$ and the inflationary spacetime: for $a(t) = H^{-1} \cosh(Ht)$, we have

$$R(t) = \sin \left(\arcsin R - 2H \arctan(e^{Ht^*}) + 2H \arctan(e^{Ht}) \right),$$

$$(II.22) \quad R_h = \sin \left(\arcsin R - 2H \arctan(e^{Ht^*}) + \pi H \right),$$

and when $a(t) = e^t$ we have

$$(II.23) \quad R(t) = \sin(\arcsin R + e^{-t^*} - e^{-t}), \quad R_h = \sin(\arcsin R + e^{-t^*}).$$

III. ASYMPTOTIC BEHAVIOURS OF SMOOTH SOLUTIONS

In this part, we investigate the asymptotic behaviour of the fields as $t \rightarrow +\infty$. We prove that the asymptotic profile $\Psi_\infty(\cdot) := \lim_{t \rightarrow \infty} \Psi(t, \cdot)$ exists when the scale factor is exponentially increasing. In the case of the De Sitter type universe $dS_4(\mathbf{K})$, and in the case of the exponentially inflating model for which $a(t) = e^t$ we are able to compute its expression, and the first terms of the asymptotic expansion, in terms of the Cauchy data. Similar results have been obtained in [2] for the steady state universe $(\mathbb{R}_t \times \mathbb{R}_x^3, ds^2 = dt^2 - e^{2t} dx^2)$ (see also [23]).

III.1. Asymptotic profile. We prove the existence of Ψ_∞ when the scale factor is at least exponentially increasing, *i.e.* satisfies an assumption of the type:

$$(III.1) \quad \exists \gamma > 0, \quad \exists t^* \in \mathbb{R}, \quad \forall t \geq t^* \quad \gamma \leq \frac{a'(t)}{a(t)}.$$

Theorem III.1. *We assume (III.1) is satisfied. Then for any finite energy solution Ψ of (I.2) there exists $\Psi_\infty \in L^2(\mathbf{K})$ such that*

$$(III.2) \quad \|\Psi(t) - \Psi_\infty\|_{L^2(\mathbf{K})} \lesssim e^{-\gamma t} E^{\frac{1}{2}}(\Psi, t^*), \quad t^* \leq t.$$

Proof. Our method relies on the spectral expansion of $\Psi(t, \cdot)$ and the energy estimate (or an explicit resolution) for the ODE. More precisely, since the Laplace-Beltrami operator $\Delta_{\mathbf{K}}$ on \mathbf{K} is a non positive, self-adjoint elliptic operator on a compact manifold, its spectrum is a discrete set of eigenvalues $-q^2 \leq 0$. Moreover, by the Hilbert-Schmidt theorem there exists an orthonormal basis in $L^2(\mathbf{K})$, formed of eigenfunctions $(\Psi_q)_q \subset H^1(\mathbf{K})$ associated to q^2 , *i.e.*

$$-\Delta_{\mathbf{K}} \Psi_q = q^2 \Psi_q.$$

Moreover the eigenvalues are explicitly known (see [1, 10, 12, 13]). One has:

$$(III.3) \quad 0 \leq q, \quad q^2 = \beta^2 - 1,$$

$$(III.4) \quad \text{with } \beta \in \{1, 13, 21, 25, 31, 33, 37, 41, 43, 45, 49, 51, 53, 55, 57\} \cup \{2n + 1, n \geq 30\}.$$

Any finite energy solution $\Psi(t, X)$ of equation (I.2) has an expansion of the form

$$(III.5) \quad \Psi(t, X) = \sum_q u_q(t) \Psi_q(X), \quad t \in \mathbb{R}, \quad X \in \mathbf{K},$$

where u_q is solution of the ordinary differential equation

$$(III.6) \quad u_q'' + 3 \frac{a'(t)}{a(t)} u_q' + \frac{q^2}{a^2(t)} u_q = 0.$$

For the finite energy solution we have

$$(III.7) \quad \sum_q \left| u_q'(t) \right|^2 + q^2 |u_q(t)|^2 < \infty,$$

and if Ψ is a smooth solution we have

$$\forall k, p \in \mathbb{N}, \quad \sum_q q^p \left| \frac{d^k}{dt^k} u_q(t) \right| < \infty.$$

These series converge locally uniformly with respect to t . Now, multiplying (III.6) by u'_q , we get an energy type equality:

$$|u'_q(t)|^2 + \frac{q^2}{a^2(t)} |u_q(t)|^2 = -2 \frac{a'(t)}{a(t)} \left(3 |u'_q(t)|^2 + \frac{q^2}{a^2(t)} |u_q(t)|^2 \right).$$

We get from hypothese (III.1) that

$$\frac{d}{dt} \left(|u'_q(t)|^2 + \frac{q^2}{a^2(t)} |u_q(t)|^2 \right) \leq -2\gamma \left(|u'_q(t)|^2 + \frac{q^2}{a^2(t)} |u_q(t)|^2 \right),$$

hence we deduce that there exists $C > 0$ independent of q such that for any $t \geq t^*$ we have:

$$(III.8) \quad |u'_q(t)| \leq C e^{-\gamma t} (|u'_q(t^*)| + q |u_q(t^*)|).$$

Therefore we can introduce

$$u_q(\infty) := u_q(t^*) + \int_{t^*}^{\infty} u'_q(t) dt, \quad \Psi_\infty := \sum_q u_q(\infty) \Psi_q.$$

Now (III.2) follows from (III.7) and (III.8). □

III.2. $d\mathcal{S}_4(\mathbf{K})$ universe. We consider the $d\mathcal{S}_4(\mathbf{K})$ universe for which $a(t) = H^{-1} \cosh(Ht)$. We calculate an explicit expression of the asymptotic profile and we prove that $\Delta_{\mathbf{K}} \Psi(t) - \frac{1}{2H} (1 - \tanh Ht)^{-1} \partial_t \Psi(t)$ tends to zero.

Theorem III.2. *Given a smooth solution Ψ of (I.2), there exist constants A_q^+ and A_q^- depending only on the initial data such that*

$$(III.9) \quad \begin{aligned} \Psi(t, X) &= \left[-\sqrt{\frac{2}{\pi}} A_0^+ + (\cosh Ht)^{-\frac{3}{2}} A_0^- P_{\frac{1}{2}}^{-\frac{3}{2}}(\tanh Ht) \right] \Psi_0(X) \\ &\quad + (\cosh Ht)^{-\frac{3}{2}} \sum_{q \neq 0} \left[A_q^+ P_{\beta - \frac{1}{2}}^{\frac{3}{2}}(\tanh Ht) + A_q^- Q_{\beta - \frac{1}{2}}^{\frac{3}{2}}(\tanh Ht) \right] \Psi_q(X), \\ \Psi_\infty(X) &= -\sqrt{\frac{2}{\pi}} \sum_q A_q^+ \Psi_q(X), \\ \Psi(t, X) - \Psi_\infty(X) &= -\sqrt{\frac{2}{\pi}} \sum_{q \neq 0} q^2 A_q^+ \Psi_q(X) (1 - \tanh Ht) + 0 \left((1 - \tanh Ht)^{\frac{3}{2}} \right), \\ \Delta_{\mathbf{K}} \Psi(t, X) - \frac{1}{2H} (1 - \tanh Ht)^{-1} \partial_t \Psi(t, X) &= \frac{2}{\sqrt{\pi}} A_0^- (1 - \tanh Ht)^{\frac{1}{2}} \\ &\quad + \sqrt{\frac{2}{\pi}} \left[\sum_{q \neq 0} q^2 \left(q^2 + \frac{3}{4} \right) A_q^+ \Psi_q(X) \right] (1 - \tanh Ht) + 0 (1 - \tanh Ht)^{\frac{3}{2}} \end{aligned}$$

where q and β are given by (III.3), (III.4).

Proof. The differential equation (III.6) has the form:

$$(III.10) \quad u_q''(t) + 3H \tanh(Ht) u_q'(t) + \frac{q^2 H^2}{\cosh^2(Ht)} u_q(t) = 0.$$

For each q we introduce a new function w_q defined by

$$u_q(t) := (\cosh Ht)^{-\frac{3}{2}} w_q(t).$$

Then u_q satisfies (III.10) iff w_q is solution of

$$(III.11) \quad H^{-2} w_q''(t) + \left((q^2 + \frac{3}{4}) \cosh^{-2}(Ht) - \frac{9}{4} \right) w_q(t) = 0.$$

Now we put $w_q(t) = \tilde{w}_q(\tanh Ht)$. Thanks to the relation $q^2 + \frac{3}{4} = (\beta - \frac{1}{2})(\beta + \frac{1}{2})$ we deduce that w_q satisfies (III.11) iff \tilde{w}_q is solution of the associated Legendre equation

$$(III.12) \quad (1 - x^2) \tilde{w}_q''(x) - 2x \tilde{w}_q'(x) + \left(\nu(\nu + 1) - \frac{\mu^2}{1 - x^2} \right) \tilde{w}_q(x) = 0,$$

where $\nu = \beta - \frac{1}{2}$, $\mu = \pm \frac{3}{2}$ and $x \in]-1, +1[$. In the sequel, we use several formulae, all from [19]. The first eigenvalue $q = 0$ is a particular case where $\nu = \frac{1}{2}$. Thanks to formula 14.2.7 the Wronskian of $P_{\frac{1}{2}}^{-\frac{3}{2}}(x)$ and $P_{\frac{1}{2}}^{\frac{3}{2}}(x)$ is not zero. For the other eigenvalues, β is greater than 13 and is an odd integer. So $Q_{\beta - \frac{1}{2}}^{\frac{3}{2}}$ is defined and, thanks to formula 14.2.4, the Wronskian of $P_{\beta - \frac{1}{2}}^{\frac{3}{2}}(x)$ and $Q_{\beta - \frac{1}{2}}^{\frac{3}{2}}(x)$ is not zero. So there exist constants A_q^+ and A_q^- depending on initial data such that

$$\tilde{w}_0(x) = A_0^+ P_{\frac{1}{2}}^{\frac{3}{2}}(x) + A_0^- P_{\frac{1}{2}}^{-\frac{3}{2}}(x), \text{ and } \tilde{w}_q(x) = A_q^+ P_{\beta - \frac{1}{2}}^{\frac{3}{2}}(x) + A_q^- Q_{\beta - \frac{1}{2}}^{\frac{3}{2}}(x) \text{ for } q \neq 0.$$

Then

$$(III.13) \quad u_0(t) = (\cosh Ht)^{-\frac{3}{2}} \left[A_0^+ P_{\frac{1}{2}}^{\frac{3}{2}}(\tanh Ht) + A_0^- P_{\frac{1}{2}}^{-\frac{3}{2}}(\tanh Ht) \right],$$

$$(III.14) \quad u_q(t) = (\cosh Ht)^{-\frac{3}{2}} \left[A_q^+ P_{\beta - \frac{1}{2}}^{\frac{3}{2}}(\tanh Ht) + A_q^- Q_{\beta - \frac{1}{2}}^{\frac{3}{2}}(\tanh Ht) \right] \text{ for } q \neq 0.$$

To obtain asymptotic profiles we use hypergeometric representation of the Ferrers functions (see formulae 14.3.i). We recall that for $x \in]-1, +1[$

$$\begin{aligned} P_{\nu}^{\mu}(x) &= \left(\frac{1+x}{1-x} \right)^{\frac{\mu}{2}} \mathbf{F}(\nu + 1, -\nu; 1 - \mu; \frac{1}{2} - \frac{1}{2}x) \\ &= \left(\frac{1+x}{1-x} \right)^{\frac{\mu}{2}} \sum_{s=0}^{+\infty} \frac{(\nu+1)_s (-\nu)_s}{\Gamma(1-\mu+s)} \frac{1}{s!} \left(\frac{1}{2} \right)^s (1-x)^s, \end{aligned}$$

where $(\alpha)_n$ is the Pochhammer's symbol: $\alpha(\alpha+1)(\alpha+2)\dots(\alpha+n-1)$ if $n = 1, 2, 3, \dots$, and 1 if $n = 0$. First we consider the case $q \neq 0$, that is $\nu = \beta - \frac{1}{2} \neq \frac{1}{2}$. For t in the neighbourhood of $+\infty$, the regularity of the previous series at 0 leads to

$$\begin{aligned} P_{\nu}^{\frac{3}{2}}(\tanh Ht) &= \left(\frac{1+\tanh Ht}{1-\tanh Ht} \right)^{\frac{3}{4}} \left[\frac{1}{\Gamma(-\frac{1}{2})} + \frac{(\nu+1)(-\nu)}{2\Gamma(\frac{1}{2})} (1 - \tanh Ht) \right. \\ &\quad \left. + \frac{(\nu+1)(\nu+2)(-\nu)(-\nu+1)}{8\Gamma(\frac{3}{2})} (1 - \tanh Ht)^2 + 0 \left((1 - \tanh Ht)^3 \right) \right]. \end{aligned}$$

So

$$(III.15) \quad (\cosh Ht)^{-\frac{3}{2}} P_{\beta-\frac{1}{2}}^{\frac{3}{2}}(\tanh Ht) = (1 + \tanh Ht)^{\frac{3}{2}} \left[\frac{1}{\Gamma(\frac{1}{2})} - (\beta^2 - \frac{1}{4}) \frac{1}{2\Gamma(\frac{1}{2})} (1 - \tanh Ht) \right. \\ \left. + \frac{(\beta^2 - \frac{1}{4})(\beta^2 - \frac{9}{4})}{8\Gamma(\frac{3}{2})} (1 - \tanh Ht)^2 + 0 \left((1 - \tanh Ht)^3 \right) \right].$$

Likewise for $x \in]-1, +1[$

$$\begin{aligned} Q_{\beta-\frac{1}{2}}^{\frac{3}{2}}(x) &= \frac{\pi}{2 \sin(\frac{3}{2}\pi)} \left(\cos(\frac{3}{2}\pi) \left(\frac{1+x}{1-x} \right)^{\frac{3}{4}} \mathbf{F}(\nu + 1, -\nu; -\frac{1}{2}; \frac{1}{2} - \frac{1}{2}x) \right. \\ &\quad \left. - \frac{\Gamma(\nu + \frac{5}{2})}{\Gamma(\nu - \frac{1}{2})} \left(\frac{1-x}{1+x} \right)^{\frac{3}{4}} \mathbf{F}(\nu + 1, -\nu; \frac{5}{2}; \frac{1}{2} - \frac{1}{2}x) \right) \\ &= \frac{\pi}{2} \frac{\Gamma(\nu + \frac{5}{2})}{\Gamma(\nu - \frac{1}{2})} \left(\frac{1-x}{1+x} \right)^{\frac{3}{4}} \sum_{s=0}^{+\infty} \frac{(\nu+1)_s (-\nu)_s}{\Gamma(\frac{5}{2}+s)} \frac{1}{s!} \left(\frac{1}{2} \right)^s (1-x)^s. \end{aligned}$$

Then, for t in the neighbourhood of $+\infty$ we have

$$(III.16) \quad Q_{\beta-\frac{1}{2}}^{\frac{3}{2}}(\tanh Ht) = \frac{\pi}{2} \frac{\Gamma(\beta + 2)}{\Gamma(\beta - 1)} \left(\frac{1 - \tanh Ht}{1 + \tanh Ht} \right)^{\frac{3}{4}} \left[\frac{1}{\Gamma(\frac{5}{2})} - (\beta^2 - \frac{1}{4}) \frac{1}{2\Gamma(\frac{7}{2})} (1 - \tanh Ht) + 0 \left((1 - \tanh Ht)^2 \right) \right],$$

and so

$$(III.16) \quad (\cosh Ht)^{-\frac{3}{2}} Q_{\beta-\frac{1}{2}}^{\frac{3}{2}}(\tanh Ht) = \frac{\pi}{2} \frac{1}{\Gamma(\frac{5}{2})} \frac{\Gamma(\beta + 2)}{\Gamma(\beta - 1)} (1 - \tanh Ht)^{\frac{3}{2}} + 0 \left((1 - \tanh Ht)^{\frac{5}{2}} \right).$$

From (III.14), (III.15) and (III.16) we deduce for $t \rightarrow +\infty$ and $q \neq 0$

$$\begin{aligned} u_q(t) &= -A_q^+ \frac{1}{2\sqrt{\pi}} (1 + \tanh Ht)^{\frac{3}{2}} - A_q^+ \frac{\sqrt{\pi}}{2} (\beta^2 - \frac{1}{4}) (1 + \tanh Ht)^{\frac{3}{2}} (1 - \tanh Ht) \\ &\quad + 0 \left((1 - \tanh Ht)^{\frac{5}{2}} \right). \end{aligned}$$

Hence we have got for $q \neq 0$

$$(III.17) \quad u_q(t) \sim -A_q^+ \sqrt{\frac{2}{\pi}}, \text{ and } u_q(t) + A_q^+ \sqrt{\frac{2}{\pi}} = -q^2 A_q^+ \sqrt{\frac{2}{\pi}} (1 - \tanh Ht) + 0 \left((1 - \tanh Ht)^{\frac{3}{2}} \right).$$

Using formula 14.10.4 we deduce derivatives of u_q from (III.14). For $q \neq 0$ we have

$$\begin{aligned} (III.18) \quad u'_q(t) &= H (\cosh Ht)^{-\frac{3}{2}} (\tanh Ht) (\beta - 1) \left[A_q^+ P_{\beta-\frac{1}{2}}^{\frac{3}{2}}(\tanh Ht) + A_q^- Q_{\beta-\frac{1}{2}}^{\frac{3}{2}}(\tanh Ht) \right] \\ &\quad - H (\cosh Ht)^{-\frac{3}{2}} (\beta - 1) \left[A_q^+ P_{\beta+\frac{1}{2}}^{\frac{3}{2}}(\tanh Ht) + A_q^- Q_{\beta+\frac{1}{2}}^{\frac{3}{2}}(\tanh Ht) \right] \\ &= H (\cosh Ht)^{-\frac{3}{2}} (\beta - 1) A_q^+ \left[(\tanh Ht) P_{\beta-\frac{1}{2}}^{\frac{3}{2}}(\tanh Ht) - P_{\beta+\frac{1}{2}}^{\frac{3}{2}}(\tanh Ht) \right] \\ &\quad + H (\cosh Ht)^{-\frac{3}{2}} (\beta - 1) A_q^- \left[(\tanh Ht) Q_{\beta-\frac{1}{2}}^{\frac{3}{2}}(\tanh Ht) - Q_{\beta+\frac{1}{2}}^{\frac{3}{2}}(\tanh Ht) \right]. \end{aligned}$$

And from (III.18), (III.15) and (III.16) we deduce for $\nu = \beta - \frac{1}{2} \neq \frac{1}{2}$ and $t \rightarrow +\infty$

$$\begin{aligned} u'_q(t) &= H(\beta - 1)A_q^+ (1 + \tanh Ht)^{\frac{3}{2}} \\ &\left[\frac{1}{\Gamma(-\frac{1}{2})} (-1 + \tanh Ht) + \left(-(\beta^2 - \frac{1}{4}) \tanh Ht + (\beta + \frac{3}{2})(\beta + \frac{1}{2}) \right) \frac{1}{2\Gamma(\frac{1}{2})} (1 - \tanh Ht) \right. \\ &\quad \left. + \left((\beta^2 - \frac{1}{4})(\beta^2 - \frac{9}{4}) \tanh Ht - (\beta + \frac{3}{2})(\beta + \frac{5}{2})(\beta^2 - \frac{1}{4}) \right) \frac{1}{8\Gamma(\frac{3}{2})} (1 - \tanh Ht)^2 \right] \\ &\quad + 0 \left((1 - \tanh Ht)^{\frac{5}{2}} \right). \end{aligned}$$

That is for $q \neq 0$

$$\begin{aligned} u'_q(t) &= A_q^+ \frac{H}{\sqrt{\pi}} (\beta^2 - 1) (1 + \tanh Ht)^{\frac{3}{2}} \\ &\quad \left[(1 - \tanh Ht) - (\beta^2 - \frac{1}{4}) (1 - \tanh Ht)^2 + 0 (1 - \tanh Ht)^{\frac{5}{2}} \right], \end{aligned}$$

and then

$$\begin{aligned} -2Hq^2 u_q(t) - (1 - \tanh Ht)^{-1} u'_q(t) &= \\ q^2 \left(q^2 + \frac{3}{4} \right) A_q^+ \frac{H}{\sqrt{\pi}} (1 + \tanh Ht)^{\frac{3}{2}} (1 - \tanh Ht) + 0 (1 - \tanh Ht)^{\frac{3}{2}}. \end{aligned}$$

It only remains to consider the case $q = 0$. Actually u_0 can be written more simply by explaining $P_{\frac{1}{2}}^{\frac{3}{2}}$. We use formula 14.10.4: $(1 - x^2) \left(P_{\frac{1}{2}}^{\frac{3}{2}} \right)'(x) = \left(\frac{3}{2} - \frac{1}{2} - 1 \right) P_{\frac{1}{2}}^{\frac{3}{2}}(x) + \frac{3}{2} x P_{\frac{1}{2}}^{\frac{3}{2}}(x) = \frac{3}{2} x P_{\frac{1}{2}}^{\frac{3}{2}}(x)$. So $P_{\frac{1}{2}}^{\frac{3}{2}}$ has the form $C (1 - x^2)^{-\frac{3}{4}}$ where C is a constant. Since $P_{\frac{1}{2}}^{\frac{3}{2}}(0) = \mathbf{F}\left(\frac{3}{2}, -\frac{1}{2}; -\frac{1}{2}; \frac{1}{2}\right) = -\sqrt{\frac{2}{\pi}}$ we can write $P_{\frac{1}{2}}^{\frac{3}{2}}(x) = -\sqrt{\frac{2}{\pi}} (1 - x^2)^{-\frac{3}{4}}$. So with (III.14) we obtain a new expression of u_0 :

$$u_0(t) = -\sqrt{\frac{2}{\pi}} A_0^+ + (\cosh Ht)^{-\frac{3}{2}} A_0^- P_{\frac{1}{2}}^{-\frac{3}{2}}(\tanh Ht).$$

Moreover the hypergeometric representation of $P_{\frac{1}{2}}^{-\frac{3}{2}}$ gives us for t at $+\infty$

$$\begin{aligned} (\cosh Ht)^{-\frac{3}{2}} P_{\frac{1}{2}}^{-\frac{3}{2}}(\tanh Ht) &= \\ (1 - \tanh Ht)^{\frac{3}{2}} \left[\frac{1}{\Gamma(\frac{5}{2})} - \frac{3}{8} \frac{1}{\Gamma(\frac{7}{2})} (1 - \tanh Ht) - \frac{15}{128} \frac{1}{\Gamma(\frac{9}{2})} (1 - \tanh Ht)^2 + 0 \left((1 - \tanh Ht)^3 \right) \right], \end{aligned}$$

so

$$(III.19) \quad u_0(t) = -\sqrt{\frac{2}{\pi}} A_0^+ + A_0^- \frac{1}{\Gamma(\frac{5}{2})} (1 - \tanh Ht)^{\frac{3}{2}} + 0 \left((1 - \tanh Ht)^{\frac{5}{2}} \right).$$

Then (III.17) and (III.19) prove (III.9). On the other hand we can simplify u'_0 since $P_{\frac{3}{2}}^{-\frac{3}{2}}$ has a simple writing (see formula 14.5.18 with $\theta \in]0, \pi[$ such that $\cos \theta = \tanh Ht$). We have:

$$\begin{aligned} u'_0(t) &= -3H (\cosh Ht)^{-\frac{3}{2}} A_0^- P_{\frac{3}{2}}^{-\frac{3}{2}}(\tanh Ht) \\ &= -3H (\cosh Ht)^{-\frac{3}{2}} \frac{1}{2^{\frac{3}{2}} \Gamma(\frac{3}{2} + 1)} A_0^- (\sin \theta)^{\frac{3}{2}} = H \sqrt{\frac{2}{\pi}} (\cosh Ht)^{-3} A_0^- \\ &= -H \sqrt{\frac{2}{\pi}} A_0^- (1 + \tanh Ht)^{\frac{3}{2}} (1 - \tanh Ht)^{\frac{3}{2}}, \end{aligned}$$

so

$$-\frac{1}{2H} (1 - \tanh Ht)^{-1} u'_0(t) = \frac{1}{\sqrt{2\pi}} A_0^- (1 + \tanh Ht)^{\frac{3}{2}} (1 - \tanh Ht)^{\frac{1}{2}}.$$

The proof is complete. \square

III.3. Inflating universe. We consider the toy model of an exponentially inflating universe with $a(t) = e^t$. We calculate the asymptotic profile of a wave Ψ and we show that $\Delta_{\mathbf{K}}\Psi(t) - e^{2t}\partial_t\Psi(t)$ tends to zero.

Theorem III.3. *Given a smooth solution Ψ of (I.2), there exist constants A_q^+ and A_q^- depending only on initial data such that*

$$(III.20) \quad \Psi(t, X) = [A_0^- e^{-3t} + A_0^+] \Psi_0(X) + e^{-\frac{3}{2}t} \sum_{q \neq 0} [A_q^- J_{\frac{3}{2}}(qe^{-t}) + A_q^+ Y_{\frac{3}{2}}(qe^{-t})] \Psi_q(X),$$

$$(III.21) \quad \begin{aligned} \Psi_\infty(X) &= A_0^+ \Psi_0(X) - \sqrt{\frac{2}{\pi}} \sum_{q \neq 0} q^{-\frac{3}{2}} A_q^+ \Psi_q(X), \\ \Psi(t, X) - \Psi_\infty(X) &= -e^{-2t} \left(\frac{1}{2} \sqrt{\frac{2}{\pi}} \sum_{q \neq 0} q^{\frac{1}{2}} A_q^+ \Psi_q(X) \right) + o(e^{-3t}), \end{aligned}$$

$$(III.22) \quad \Delta_{\mathbf{K}}\Psi(t, X) - e^{2t}\partial_t\Psi(t, X) = e^{-t} \left(3A_0^- \Psi_0(X) + \sqrt{\frac{2}{\pi}} \sum_{q \neq 0} q^{\frac{3}{2}} A_q^- \Psi_q(X) \right) + o(e^{-2t})$$

where the set of q is given by (III.3), (III.4).

Proof. When $a(t) = e^t$, equation (III.6) is just

$$(III.23) \quad u_q''(t) + 3u_q'(t) + q^2 e^{-2t} u_q = 0.$$

For each q we introduce a new function w_q defined by

$$u_q(t) := e^{-\frac{3}{2}t} w_q(t).$$

Then u_q satisfies (III.23) iff w_q is solution of

$$(III.24) \quad w_q''(t) + \left(q^2 e^{-2t} - \frac{9}{4} \right) w_q = 0.$$

$q = 0$ is a particular case. w_0 can be written $w_0(t) = A_0^- e^{-\frac{3}{2}t} + A_0^+ e^{+\frac{3}{2}t}$ where A_0^+ and A_0^- are constants depending on initial data. So

$$(III.25) \quad u_0(t) = A_0^- e^{-3t} + A_0^+.$$

Then we consider $q \neq 0$ and we put $w_q(t) = \tilde{w}_q(qe^{-t})$. w_q satisfies (III.24) iff \tilde{w}_q is solution of the Bessel equation

$$(III.26) \quad x^2 \tilde{w}_q''(x) + x \tilde{w}_q'(x) + \left(x^2 - \left(\frac{3}{2} \right)^2 \right) \tilde{w}_q(x) = 0.$$

For x belonging to $]0, +\infty[$, \tilde{w}_q can be written $\tilde{w}_q(x) = A_q^+ Y_{\frac{3}{2}}(x) + A_q^- J_{\frac{3}{2}}(x)$ where A_q^- and A_q^+ are constants depending on initial data (see 10.2 of [19]). So we have

$$u_q(t) = e^{-\frac{3}{2}t} A_q^- J_{\frac{3}{2}}(qe^{-t}) + e^{-\frac{3}{2}t} A_q^+ Y_{\frac{3}{2}}(qe^{-t}).$$

According to 10.6.2 ([19]) the derivatives of $J_{\frac{3}{2}}$ and $Y_{\frac{3}{2}}$ satisfy $C_{\frac{3}{2}}'(x) = C_{\frac{1}{2}}(x) - \frac{3}{2x} C_{\frac{3}{2}}(x)$. We obtain

$$\begin{aligned} u_q'(t) &= -e^{-\frac{3}{2}t} \left[\frac{3}{2} A_q^- J_{\frac{3}{2}}(qe^{-t}) + qe^{-t} A_q^- J_{\frac{3}{2}}'(qe^{-t}) + \frac{3}{2} A_q^+ Y_{\frac{3}{2}}(qe^{-t}) + qe^{-t} A_q^+ Y_{\frac{3}{2}}'(qe^{-t}) \right] \\ &= -e^{-\frac{5}{2}t} q A_q^- J_{\frac{1}{2}}(qe^{-t}) - e^{-\frac{5}{2}t} q A_q^+ Y_{\frac{1}{2}}(qe^{-t}). \end{aligned}$$

In fact, by the use of some formulae in 10.47ii and 10.49i, these Bessel functions have simple expressions:

$$\begin{aligned} J_{\frac{1}{2}}(x) &= \sqrt{\frac{2x}{\pi}} j_0(x) = \sqrt{\frac{2}{\pi x}} \sin x, & Y_{\frac{1}{2}}(x) &= \sqrt{\frac{2x}{\pi}} y_0(x) = -\sqrt{\frac{2}{\pi x}} \cos x, \\ J_{\frac{3}{2}}(x) &= \sqrt{\frac{2x}{\pi}} j_1(x) = \sqrt{\frac{2x}{\pi}} \left[\frac{\sin x}{x^2} - \frac{\cos x}{x} \right], & Y_{\frac{3}{2}}(x) &= \sqrt{\frac{2x}{\pi}} y_1(x) = \sqrt{\frac{2x}{\pi}} \left[-\frac{\cos x}{x^2} - \frac{\sin x}{x} \right]. \end{aligned}$$

To investigate the behaviour of u_q at $+\infty$ we use the following asymptotics at 0 of $Y_{\frac{3}{2}}$, $J_{\frac{3}{2}}$, $Y_{\frac{1}{2}}$ and $J_{\frac{1}{2}}$.

$$\begin{aligned} J_{\frac{1}{2}}(x) &= \sqrt{\frac{2}{\pi}} \left[x^{\frac{1}{2}} - \frac{1}{6} x^{\frac{5}{2}} + \frac{1}{120} x^{\frac{9}{2}} + O(x^{\frac{13}{2}}) \right], \\ Y_{\frac{1}{2}}(x) &= \sqrt{\frac{2}{\pi}} \left[-x^{-\frac{1}{2}} + \frac{1}{2} x^{\frac{3}{2}} - \frac{1}{24} x^{\frac{7}{2}} + \frac{1}{720} x^{\frac{11}{2}} + O(x^{\frac{15}{2}}) \right], \\ J_{\frac{3}{2}}(x) &= \sqrt{\frac{2}{\pi}} \left[\frac{1}{3} x^{\frac{3}{2}} - \frac{1}{30} x^{\frac{7}{2}} + \frac{1}{840} x^{\frac{11}{2}} + O(x^{\frac{15}{2}}) \right], \\ Y_{\frac{3}{2}}(x) &= \sqrt{\frac{2}{\pi}} \left[-x^{-\frac{3}{2}} - \frac{1}{2} x^{\frac{1}{2}} + \frac{1}{8} x^{\frac{5}{2}} - \frac{1}{144} x^{\frac{9}{2}} + O(x^{\frac{13}{2}}) \right]. \end{aligned}$$

All these relations show that for any $q \neq 0$ we have at $+\infty$

$$\begin{aligned} u_q(t) &= \sqrt{\frac{2}{\pi}} e^{-\frac{3}{2}t} A_q^- \left[\frac{1}{3} (qe^{-t})^{\frac{3}{2}} \right] + \\ &\quad \sqrt{\frac{2}{\pi}} e^{-\frac{3}{2}t} A_q^+ \left[- (qe^{-t})^{-\frac{3}{2}} - \frac{1}{2} (qe^{-t})^{\frac{1}{2}} + \frac{1}{8} (qe^{-t})^{\frac{5}{2}} \right] + 0(e^{-4t}) \\ &= \sqrt{\frac{2}{\pi}} \left[-q^{-\frac{3}{2}} A_q^+ - \frac{1}{2} q^{\frac{1}{2}} A_q^+ e^{-2t} + \frac{1}{3} q^{\frac{3}{2}} A_q^- e^{-3t} \right] + 0(e^{-4t}), \end{aligned}$$

and

$$(III.27) \quad u'_q(t) = -e^{-\frac{5}{2}t} q \sqrt{\frac{2}{\pi}} A_q^- (qe^{-t})^{\frac{1}{2}} + e^{-\frac{5}{2}t} q \sqrt{\frac{2}{\pi}} A_q^+ (qe^{-t})^{-\frac{1}{2}} + 0(e^{-4t})$$

$$(III.28) \quad = \sqrt{\frac{2}{\pi}} \left[q^{\frac{1}{2}} A_q^+ e^{-2t} - q^{\frac{3}{2}} A_q^- e^{-3t} \right] + 0(e^{-4t}).$$

(III.21) is proved thanks to (III.25) and (III.27). Moreover for all $q \neq 0$ (III.28) gives

$$\begin{aligned} -q^2 u_q(t) - e^{2t} u'_q(t) &= \sqrt{\frac{2}{\pi}} q^{\frac{1}{2}} A_q^+ - \sqrt{\frac{2}{\pi}} \left[q^{\frac{1}{2}} A_q^+ - q^{\frac{3}{2}} A_q^- e^{-t} \right] + 0(e^{-2t}) \\ &= \sqrt{\frac{2}{\pi}} q^{\frac{3}{2}} A_q^- e^{-t} + 0(e^{-2t}). \end{aligned}$$

Then, thanks to (III.25), we deduce

$$\begin{aligned} \Delta_{\mathbf{K}} \Psi(t, X) - e^{2t} \partial_t \Psi(t, X) &= -e^{2t} u'_0(t) \Psi_0(X) + \sum_{q \neq 0} \left(-q^2 u_q(t) - e^{2t} u'_q(t) \right) \Psi_q(X) \\ &= (3A_0^- \Psi_0(X)) e^{-t} + \left(\sqrt{\frac{2}{\pi}} \sum_{q \neq 0} q^{\frac{3}{2}} A_q^- \Psi_q(X) \right) e^{-t} + 0(e^{-2t}). \end{aligned}$$

This achieves the proof. □

IV. NUMERICAL RESOLUTION

We develop in this part an accurate scheme of computation of the wave propagating on \mathbf{K} in both cases $a(t) = H^{-1} \cosh(Ht)$ and $a(t) = e^t$. The computations are performed on \mathcal{F}_v . The precise computation during a long time is a hard task because of the exponential behaviour of the scale factor. To overcome this difficulty we use finite elements of second order. The validity of our approach is established by numerically checking the asymptotic results of the previous section.

We solve the variational problem (II.17) using the usual way (see *e.g.* [6]). We take a family V_h , $0 < h \leq h_0$, of finite dimensional vector subspaces of $W^1(\mathcal{F}_v)$. We assume that

$$\overline{\cup_{0 < h \leq h_0} V_h} = W^1(\mathcal{F}_v).$$

We choose sequences $u_{0,h}$, $u_{1,h} \in V_h$ such that

$$u_{0,h} \rightarrow u_0 \text{ in } W^1(\mathcal{F}_v), \quad u_{1,h} \rightarrow u_1 \text{ in } L^2(\mathcal{F}_v).$$

We consider the solution $u_h \in C^\infty(\mathbb{R}_t; V_h)$ of

$$\begin{aligned} \forall \phi_h \in V_h, \quad 0 &= \frac{d^2}{dt^2} \int_{\mathcal{F}_v} (1 - |X|^2)^{-\frac{1}{2}} u_h(t, X) \phi_h(X) dX \\ &+ 3 \frac{a'(t)}{a(t)} \frac{d}{dt} \int_{\mathcal{F}_v} (1 - |X|^2)^{-\frac{1}{2}} u_h(t, X) \phi_h(X) dX \\ &+ \frac{1}{a^2(t)} \int_{\mathcal{F}_v} (1 - |X|^2)^{-\frac{1}{2}} \nabla u_h(t, X) \cdot \nabla \phi_h(t, X) dX \\ &- \frac{1}{a^2(t)} \int_{\mathcal{F}_v} (1 - |X|^2)^{-\frac{1}{2}} (X \cdot \nabla u_h(t, X)) (X \cdot \nabla \phi_h(t, X)) dX, \end{aligned}$$

satisfying $u_h(t^*, \cdot) = u_{0,h}(\cdot)$, $\partial_t u_h(t^*, \cdot) = u_{1,h}(\cdot)$. We shall put an initial data at $t = t^*$ with t^* large enough, rather than at $t = 0$, in order to achieve faster limit states. We consider a

basis $(e_j^h)_{1 \leq j \leq N_h}$ of V_h and we expand u_h on this basis:

$$u_h(t) = \sum_{j=1}^{N_h} u_j^h(t) e_j^h.$$

We introduce

$$U(t) := {}^t(u_1^h, u_2^h, \dots, u_{N_h}^h), \quad \mathbb{M} = (M_{ij})_{1 \leq i, j \leq N_h}, \quad \mathbb{D} = (D_{ij})_{1 \leq i, j \leq N_h}, \quad \mathbb{K} = (K_{ij})_{1 \leq i, j \leq N_h}$$

where

$$\begin{aligned} M_{ij} &:= \int_{\mathcal{F}_v} \frac{1}{\sqrt{1-|X|^2}} e_i^h(X) e_j^h(X) dX, \\ K_{ij} &:= \int_{\mathcal{F}_v} \frac{1}{\sqrt{1-|X|^2}} (\partial_x e_i^h(X) \partial_x e_j^h(X) + \partial_y e_i^h(X) \partial_y e_j^h(X) + \partial_z e_i^h(X) \partial_z e_j^h(X)) dX, \\ D_{ij} &:= (x \partial_x e_j^h(X) + y \partial_y e_j^h(X) + z \partial_z e_j^h(X)) dX. \end{aligned}$$

Then the variational formulation is equivalent to

$$(IV.1) \quad \mathbb{M} \left(U'' + 3 \frac{a'(t)}{a(t)} U' \right) + \frac{1}{a^2(t)} (\mathbb{K} + \mathbb{D}) U = 0.$$

Like in [3] we can prove that the solution u_h obtained by solving (IV.1) tends to the solution u of (II.17) as $h \rightarrow 0$. This differential system is solved very simply by iteration by solving

$$\begin{aligned} 0 = \mathbb{M} (U^{n+1} - 2U^n + U^{n-1}) &+ 3 \frac{a'(t^* + n\Delta T)}{a(t^* + n\Delta T)} \Delta T \mathbb{M} \left(\frac{U^{n+1} - U^{n-1}}{2} \right) \\ &+ (\Delta T)^2 \frac{1}{a^2(t^* + n\Delta T)} (\mathbb{K} + \mathbb{D}) U^n \end{aligned}$$

with an initial data at t^* . The Lax-Richtmyer theorem assures that the approximate solution given by this scheme tends to u_h when the time step $\Delta T \rightarrow 0$. Moreover we compute $E_d(t^* + n\Delta T)$, an approximation at time $t^* + n\Delta T$ of the energy $E(t^* + n\Delta T)$:

$$(IV.2) \quad E_d(t^* + n\Delta T) := \left\langle \mathbb{M} \frac{U^n - U^{n-1}}{\Delta t}, \frac{U^n - U^{n-1}}{\Delta t} \right\rangle + \frac{1}{a^2(t^* + n\Delta T)} \langle (\mathbb{K} + \mathbb{D}) U^{n-1}, U^n \rangle.$$

We use the same mesh as in our previous article [3]. But we construct the finite element spaces V_h of \mathbb{P}_2 type instead of \mathbb{P}_1 type. We perform this choice to gain a better accuracy that is necessary to overcome the difficulty linked to the exponential behaviour of $a(t)$. We take into account the boundary condition (II.11) in the definition of the finite elements, so that $V_h \subset W^1(\mathcal{F}_v)$. We note \mathcal{T}_h the set of all tetrahedra of the mesh, $\mathcal{F}_{v,h}$ the set $\cup_{T \in \mathcal{T}_h} T$, and $\mathbb{P}_2(T)$ the set of second degree polynomial functions on T . We choose P_2 Lagrange finite elements, so our nodes are among vertices and middle of edges of $T \in \mathcal{T}_h$. In our construction of the mesh we took care that vertices belonging to $\partial(\mathcal{F}_{v,h})$ belong to $\partial(\mathcal{F}_v)$ and that for any vertex S of $T \in \mathcal{T}_h$, S' is also a vertex of a tetrahedron of \mathcal{T}_h if $S' \sim S$ (see [3]). It is therefore easy to take into account the boundary condition for vertices of $T \in \mathcal{T}_h$. Moreover middle of edges of peripheral tetrahedra are not on the border of \mathcal{F}_v thanks to the convexity of edges and faces of \mathcal{F}_v ; so they are only equivalent to themselves. Then we introduce:

$$V_h := \left\{ v : \mathcal{F}_{v,h} \rightarrow \mathbb{R}, v \in \mathcal{C}^0(\mathcal{F}_{v,h}), \forall T \in \mathcal{T}_h, v|_T \in \mathbb{P}_2(T), M \sim M' \Rightarrow v(M) = v(M') \right\}.$$

$\dim V_h$ is equal to the number of equivalence classes of vertices plus middle of edges of tetrahedra of \mathcal{T}_h . If j is the number of a node associated to a vertex M_j or to the middle A_j of

an edge, we construct a basis $(e_j^h)_{1 \leq j \leq N_h}$ of V_h by:

- (1) If j is associated to a node M_j that does not belong to $\partial\mathcal{F}_v$: $e_j^h(M_i) = \delta_{ij}$, $e_j^h(A_i) = 0$.
There are n_{vi} functions of this kind.
- (2) If j is associated to a node M_j that is a vertex of \mathcal{F}_v :
$$e_j^h(M_i) = \begin{cases} 1 & \text{if } M_i \sim M_j, \\ 0 & \text{otherwise} \end{cases}, \quad e_j^h(A_i) = 0.$$
There are five functions of this kind.
- (3) If j is associated to a node M_j that belongs to a face of $\partial\mathcal{F}_v$ and not to an edge:
$$e_j^h(M_i) = \begin{cases} 1 & \text{if } M_i = P_i, \\ 0 & \text{otherwise} \end{cases}, \quad e_j^h(A_i) = 0.$$
There are $6 \times n_{vf}$ functions of this kind.
- (4) If j is associated to a node M_j that belongs to an edge of a face of $\partial\mathcal{F}_v$ and is not a vertex of \mathcal{F}_v : $e_j^h(M_i) = \begin{cases} 1 & \text{if } M_i = P_i, \\ 0 & \text{otherwise} \end{cases}, \quad e_j^h(A_i) = 0.$ There are $10 \times n_{ve}$ functions of this last kind.
- (5) If j is associated to a node A_j that is a middle of an edge: $e_j^h(A_i) = \delta_{ij}$, $e_j^h(M_i) = 0$.
There are as many functions of this kind as different edges in the mesh.

with n_{ve} the number of mesh vertices on an edge of a face that are not a vertex of \mathcal{F}_v , n_{vf} the number of mesh vertices on a face that are not on an edge and n_{vi} the number of mesh vertices in $\overset{\circ}{\mathcal{F}}_v$. For a given mesh, the number of nodes is important. For example if we have a mesh with 89 vertices on each edge of \mathcal{F}_v , we have 730 309 nodes for \mathbb{P}_1 type finite elements method, and 6 377 052 nodes for \mathbb{P}_2 type method. Matrices are created with a 31 points tetrahedral quadrature formula which is of degree 7 ([11]).

With our choice of finite elements, the Laplacian is constant in a tetrahedron T ; in the following it will be noted $\Delta_{\mathcal{F}_v} u_{h|T}(t, G_T)$ where G_T is the gravity center of tetrahedron T . To test (III.10) and (III.22) we have chosen to calculate *Norm* defined respectively by:

$$Norm := \left[\sum_{T \in \mathcal{T}_h} \int_T \frac{1}{\sqrt{1 - |X|^2}} \left(\Delta_{\mathcal{F}_v} u_{h|T}(t, G_T) - \frac{1}{2H} (1 - \tanh Ht)^{-1} \partial_t u_h(t, G_T) \right)^2 dX \right]^{\frac{1}{2}}$$

and

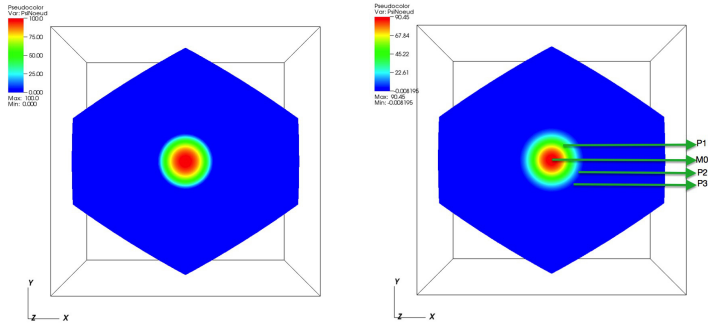
$$Norm := \left[\sum_{T \in \mathcal{T}_h} \int_T \frac{1}{\sqrt{1 - |X|^2}} \left(\Delta_{\mathcal{F}_v} u_{h|T}(t, G_T) - e^{2t} \partial_t u_h(t, G_T) \right)^2 dX \right]^{\frac{1}{2}}.$$

IV.1. Numerical results for the exponentially inflating universe. For this model the scale factor is $a(t) = e^t$. We choose different initial data and a small time step: 0.00015. We present our results for two initial data at time t^* denoted $Init_1$ and $Init_2$, of the form:

$$(IV.3) \quad u_0(X) = 100e^{\frac{d^2(X,0)}{d^2(X,0) - R_0^2}}, \quad \text{for } d(X,0) < R_0, \quad \text{and } u_0(X) = 0, \quad \text{for } d(X,0) \geq R_0.$$

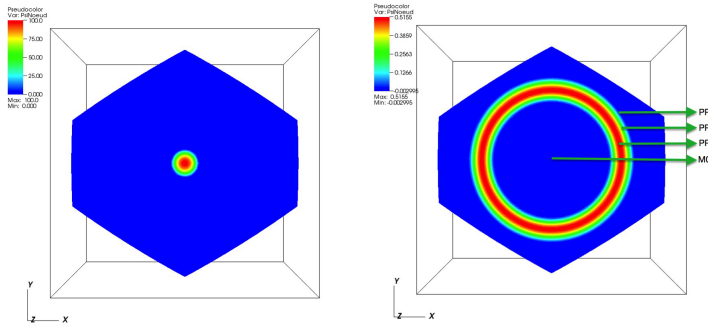
For $Init_1$ we have $R_0 = 0.1$ and for $Init_2$, $R_0 = 0.05$. In order to simplify we choose $\partial_t u(t^*, \cdot) = u_1(\cdot) = 0$. Figure 2 and figure 3 present the initial data and the limit state on the slice $z = 0$ of \mathcal{F}_v . Figure 4 shows the time evolution of the solution associated to $Init_1$ for some points P of \mathcal{F}_v pointed out in figure 2, and figure 5 shows the time evolution of

the solution associated to $Init_2$ for some point PP of \mathcal{F}_v pointed out in figure 3. In the following, $M0$ denotes a node of the mesh that is the closest to the center 0 of \mathcal{F}_v .



There is a horizon and $R_h = \sin(\arcsin 0.1 + e^{-3.5}) \simeq 0.13$.

FIGURE 2. $Init_1 : R_0 = 0.1, t^* = 3.5$.



In this case we do have $R_h = \sin(\arcsin 0.05 + e^{-1.5}) \simeq 0.27$.

FIGURE 3. $Init_2 : R_0 = 0.05, t^* = 1.5$.

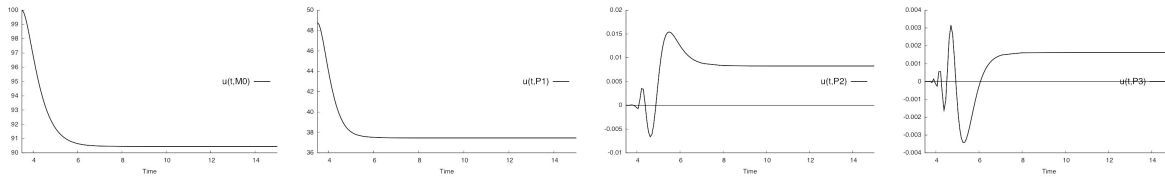


FIGURE 4. The solution $u(t, X)$ at $M0, P1, P2, P3$ with $Init_1$ and $t^* = 3.5$.

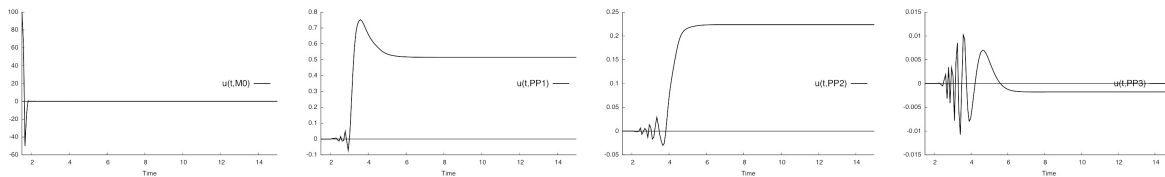


FIGURE 5. The solution $u(t, X)$ at $M0, PP1, PP2, PP3$ with $Init_2$ and $t^* = 1.5$.

It clearly appears that a limit state is reached very quickly, as soon as $t = 8$ in both cases. We also note the existence of a horizon. In table 1 and table 2 we can read the distance between previous points $M(x_M, y_M, z_M)$ of \mathcal{F}_v and its center. The agreement between the

Point	$d(0_{\mathbb{R}^3}, M)$	$u(15, M)$
M0	0.00008	90.45
P1	$0.064 < R$	37.47
P2	$0.126 \leq R_h$	0.008
P3	$0.131 \simeq R_h$	0.0016

TABLE 1. $Init_1$ and $t^* = 3.5$, $R_h \simeq 0.1299$

Point	$d(0_{\mathbb{R}^3}, M)$	$u(15, M)$
M0	$0.00008 < R$	0.0032
PP1	$R < 0.218 < R_h$	0.51
PP2	$R < 0.245 < R_h$	0.22
PP3	$R < 0.270 \simeq R_h$	-0.0017

TABLE 2. $Init_2$ and $t^* = 1.5$, $R_h \simeq 0.2697$

value of R_h given by (II.23), (II.22) is quite good, but it is difficult to have a precise numerical estimation of this horizon; for example P2 and P3 belong to a same tetrahedron, so the theoretical horizon passes through this tetrahedron. For $Init_1$ and $t^* = 3.5$ it is found that outside the ball of radius 0.129 the solution is always less than 0.01, and outside the ball of radius 0.142 the solution is always less than 0.001. Knowing that the limit state reaches 90 we conclude that the numerical estimation of R_h is satisfactory.

For large time, the time derivative becomes smaller and smaller, so the energy continues decreasing and there is no longer evolution even to $t = 30$. E_d defined by (IV.2) is decreasing. For example for $Init_2$ and $t^* = 1.5$ we have obtained:

Time t	$E_d(t)$	Time t	$E_d(t)$	Time t	$E_d(t)$	Time t	$E_d(t)$	Time t	$E_d(t)$
$t^* = 1.5$	217.16	3	0.56	4.8	$1. \cdot 10^{-3}$	11	$2.5 \cdot 10^{-9}$	19.5	10^{-16}

The test of the asymptotic behaviour (III.22) is presented in figure 6 where we note that $Norm$ is rapidly decreasing until $t = 10$. We emphasize that the exponential growth of the

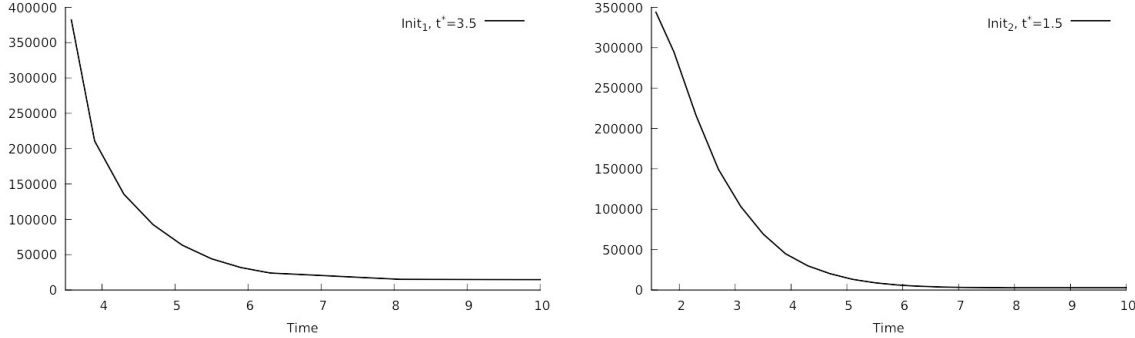
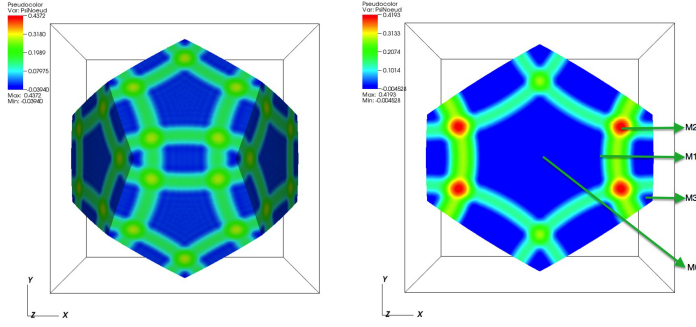


FIGURE 6. $Norm$ with respect to time

coefficients makes the computations very difficult, and this test shows the robustness of our numerical method.

IV.2. Numerical results for $dS_4(\mathbf{K})$. We assume the Hubble constant is equal to 1 hence the scale factor is $a(t) = \cosh(t)$. First we take initial data $Init_2$ and $\partial_t u(t^*, \cdot) = 0$, with $t^* = 1.5$; This is the initial data presented in the first picture of figure 3. Results are presented in figure 7 and figure 8. Figure 7 shows the limit state on the boundary of the dodecahedron, $\partial \mathcal{F}_v$, and in its interior, on the slice $z = 0$. Figure 8 shows the time evolution of the solution at some points M of \mathcal{F}_v depicted in figure 7. There is no horizon and the support of the solution is the whole \mathcal{F}_v for t large enough. R_h is equal to $\sin(\arcsin 0.05 - 2 \arctan(e^{1.5}) + \pi) \sim 0.469$ which is greater than $\sin(d_{max}) \simeq 0.378$.



We see that there exists a limit state but there is no horizon.

FIGURE 7. Limit state for $Init_2$ and $t^* = 1.5$.

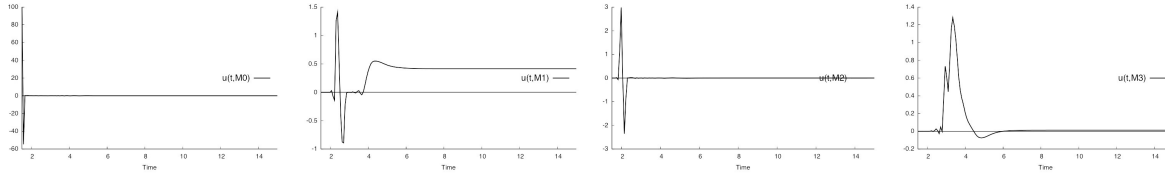
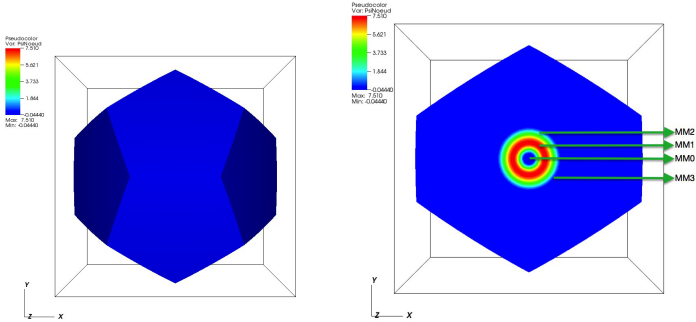


FIGURE 8
Solution $u(t, X)$ with initial data $Init_2$ at $t^* = 1.5$.

In order to see a horizon we keep the same initial data and we just modify t^* , taking $t^* = 3.5$ instead of 1.5. Then $R_h \simeq 0.11$. Results are presented in figure 9 and figure 10. Figure 9 shows that the limit state is supported inside the dodecahedron. Figure 10 presents the time evolution of the solution at some points MM of \mathcal{F}_v depicted in figure 9. In table 3 and table 4 we can read the distance between previous points $M(x_M, y_M, z_M)$ of \mathcal{F}_v and its center, and all these numerical results are in good agreement with the theoretical results on the horizon and the asymptotic profile.



There is a horizon and $R_h = \sin(\arcsin 0.05 - 2 \arctan(e^{3.5}) + \pi) \simeq 0.11$.

FIGURE 9. Limit state for $Init_2(R_0 = 0.05)$ and $t^* = 3.5$.

As for $a(t) = e^t$ we see that the limit state is quickly reached: as soon as $t = 9$ in both cases. E_d defined by (IV.2) is decreasing as we can see for example for $Init_2$ and $t^* = 1.5$:

Time t	$E_d(t)$	Time t	$E_d(t)$	Time t	$E_d(t)$	Time t	$E_d(t)$	Time t	$E_d(t)$
$t^* = 1.5$	4361	3.4	0.49	5	$1.2 \cdot 10^{-3}$	11.5	10^{-9}	19.6	$9 \cdot 10^{-17}$

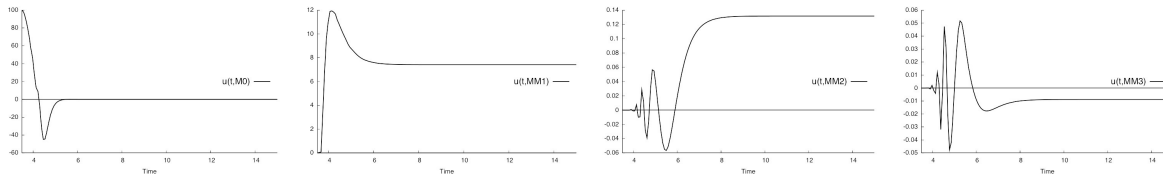


FIGURE 10
Solution $u(t, X)$ with initial data $Init_2$ at $t^* = 3.5$.

Point	$d(0_{\mathbb{R}^3}, M)$	$u(15, M)$
M0	0.00008	-0.0005
M1	0.270	0.415
M2	0.182	0.004
M3	0.354	0.013

TABLE 3. $Init_2$ and $t^* = 1.5$, no horizon.

Point	$d(0_{\mathbb{R}^3}, M)$	$u(15, M)$
$M0$	0.00008	-0.016
$MM1$	0.0544	7.41
$MM2$	0.1004	0.131
$MM3$	0.1055	-0.008

TABLE 4. $Init_2$ and $t^* = 3.5$, $R_h \simeq 0.11$

In all cases the quantity $Norm$ that tests (III.10) quickly tends to zero. On figure 11 we remark that for $t^* = 1.5$ $Norm$ is decreasing except when the support of the solution reaches the border of \mathcal{F}_v at $t \simeq 2.3$.

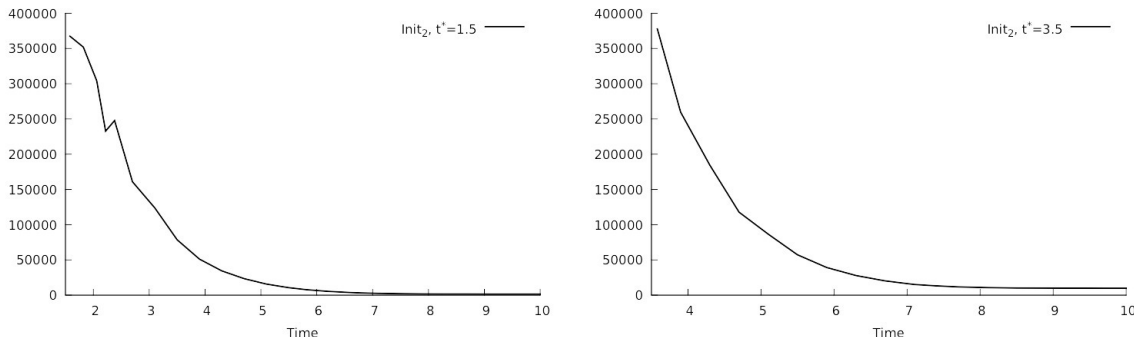


FIGURE 11. $Norm$ with respect to time

As for $a(t) = e^t$, the tests of (III.10) by the computation of $Norm$ prove that our numerical scheme is accurate and robust.

V. CONCLUSION

In this paper we have considered models of dynamical spacetimes for which the spatial section is the Poincaré dodecahedron. We have solved the Cauchy problem for the D'Alembertian and expressed the initial value problem in terms of variational formulation put on the fundamental domain. We have established the existence of an asymptotic state at the time infinity for the finite energy waves. We have obtained the analytic expression of this limit state for two important cases of accelerating universes associated to the scale factors $H^{-1} \cosh(Ht)$ and e^t . We have performed a computational method using the \mathbb{P}_2 type finite elements. The numerical experiments show a good agreement with the theoretical results on

the asymptotic behaviours. That proves the robustness and the accuracy of our method. Its drawback is the length of the computation, usually we need one week to go from t to $t + 1.2$ and this time of calculation would explode for a very refined mesh. We can hope to be able to use a parallel computing together with a domain decomposition on a significantly refined mesh.

ACKNOWLEDGEMENT

This research was partly supported by the ANR funding ANR-12-BS01-012-01.

APPENDIX

This appendix is devoted to a brief description of \mathcal{F} and \mathcal{F}_v . For more details on the construction of these domains we refer to [3].

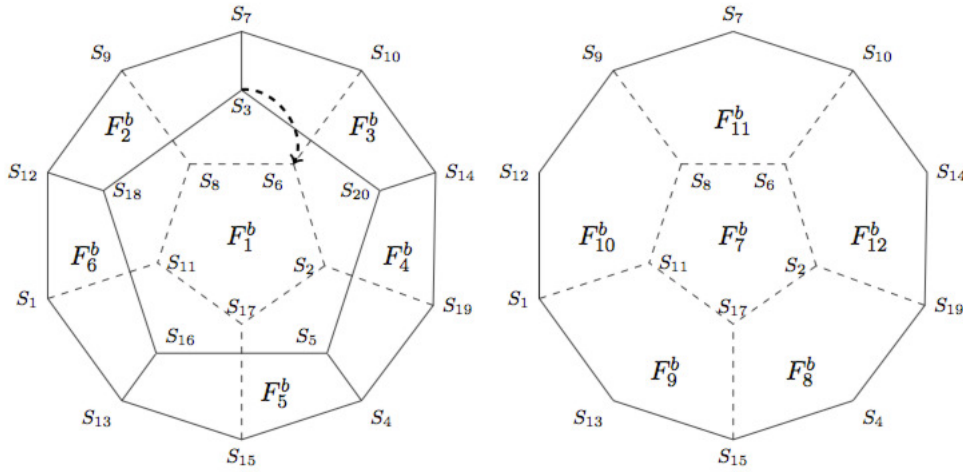


FIGURE 12. Diagram of vertices S_i , edges and faces of \mathcal{F}_v .

We warn that Figure 12 is not a faithful representation of \mathcal{F}_v as, for convenience, we have replaced the true curved faces of \mathcal{F}_v by the plane faces F_i^b that are the projection on \mathbb{R}^3 of the sets of all barycenters in \mathbb{R}^4 of the vertices S_i^1, \dots, S_i^5 of the faces F_i of \mathcal{F} .

We need the four basic quaternions $\{\mathbf{1}, \mathbf{i}, \mathbf{j}, \mathbf{k}\}$ of the set \mathbb{H} of all quaternions to define the twelve Clifford translations g_i involved in the construction of \mathcal{F} :

$$\begin{aligned}
 g_1 &:= \frac{1}{2}\sigma\mathbf{1} + \frac{1}{2}\frac{1}{\sigma}\mathbf{i} + \frac{1}{2}\mathbf{j}, & g_2 &:= \frac{1}{2}\sigma\mathbf{1} + \frac{1}{2}\mathbf{i} - \frac{1}{2}\frac{1}{\sigma}\mathbf{k}, & g_3 &:= \frac{1}{2}\sigma\mathbf{1} + \frac{1}{2}\frac{1}{\sigma}\mathbf{j} - \frac{1}{2}\mathbf{k}, \\
 g_4 &:= \frac{1}{2}\sigma\mathbf{1} - \frac{1}{2}\frac{1}{\sigma}\mathbf{i} + \frac{1}{2}\mathbf{j}, & g_5 &:= \frac{1}{2}\sigma\mathbf{1} + \frac{1}{2}\frac{1}{\sigma}\mathbf{j} + \frac{1}{2}\mathbf{k}, & g_6 &:= \frac{1}{2}\sigma\mathbf{1} + \frac{1}{2}\mathbf{i} + \frac{1}{2}\frac{1}{\sigma}\mathbf{k}.
 \end{aligned}$$

They are such that: $\forall i \in \{1, \dots, 6\}$, $g_i(F_i) = F_{i+6}$. The inverses of these six first translations are the six other translations:

$$\begin{aligned} g_7 &:= (g_1)^{-1} = \frac{1}{2}\sigma\mathbf{1} - \frac{1}{2}\frac{1}{\sigma}\mathbf{i} - \frac{1}{2}\mathbf{j}, & g_8 &:= (g_2)^{-1} = \frac{1}{2}\sigma\mathbf{1} - \frac{1}{2}\mathbf{i} + \frac{1}{2}\frac{1}{\sigma}\mathbf{k}, \\ g_9 &:= (g_3)^{-1} = \frac{1}{2}\sigma\mathbf{1} - \frac{1}{2}\frac{1}{\sigma}\mathbf{j} + \frac{1}{2}\mathbf{k}, & g_{10} &:= (g_4)^{-1} = \frac{1}{2}\sigma\mathbf{1} + \frac{1}{2}\frac{1}{\sigma}\mathbf{i} - \frac{1}{2}\mathbf{j}, \\ g_{11} &:= (g_5)^{-1} = \frac{1}{2}\sigma\mathbf{1} - \frac{1}{2}\frac{1}{\sigma}\mathbf{j} - \frac{1}{2}\mathbf{k}, & g_{12} &:= (g_6)^{-1} = \frac{1}{2}\sigma\mathbf{1} - \frac{1}{2}\mathbf{i} - \frac{1}{2}\frac{1}{\sigma}\mathbf{k}. \end{aligned}$$

(1) Coordinates of the vertices S_i of \mathcal{F} :

$$\begin{aligned} S_1 &= \frac{1}{2\sqrt{2}} \left(\sigma^2, -\frac{1}{\sigma}, \frac{1}{\sigma}, -\frac{1}{\sigma} \right), & S_2 &= \frac{1}{2\sqrt{2}} \left(\sigma^2, 1, \frac{1}{\sigma^2}, 0 \right), \\ S_3 &= \frac{1}{2\sqrt{2}} \left(\sigma^2, -\frac{1}{\sigma}, -\frac{1}{\sigma}, \frac{1}{\sigma} \right), & S_4 &= \frac{1}{2\sqrt{2}} \left(\sigma^2, \frac{1}{\sigma}, -\frac{1}{\sigma}, -\frac{1}{\sigma} \right), \\ S_5 &= \frac{1}{2\sqrt{2}} \left(\sigma^2, 0, -1, -\frac{1}{\sigma^2} \right), & S_6 &= \frac{1}{2\sqrt{2}} \left(\sigma^2, \frac{1}{\sigma}, \frac{1}{\sigma}, \frac{1}{\sigma} \right), \\ S_7 &= \frac{1}{2\sqrt{2}} \left(\sigma^2, -\frac{1}{\sigma^2}, 0, 1 \right), & S_8 &= \frac{1}{2\sqrt{2}} \left(\sigma^2, 0, 1, \frac{1}{\sigma^2} \right), \\ S_9 &= \frac{1}{2\sqrt{2}} \left(\sigma^2, -\frac{1}{\sigma}, \frac{1}{\sigma}, \frac{1}{\sigma} \right), & S_{10} &= \frac{1}{2\sqrt{2}} \left(\sigma^2, \frac{1}{\sigma^2}, 0, 1 \right), \\ S_{11} &= \frac{1}{2\sqrt{2}} \left(\sigma^2, 0, 1, -\frac{1}{\sigma^2} \right), & S_{12} &= \frac{1}{2\sqrt{2}} \left(\sigma^2, -1, \frac{1}{\sigma^2}, 0 \right), \\ S_{13} &= \frac{1}{2\sqrt{2}} \left(\sigma^2, -\frac{1}{\sigma^2}, 0, -1 \right), & S_{14} &= \frac{1}{2\sqrt{2}} \left(\sigma^2, \frac{1}{\sigma}, -\frac{1}{\sigma}, \frac{1}{\sigma} \right), \\ S_{15} &= \frac{1}{2\sqrt{2}} \left(\sigma^2, \frac{1}{\sigma^2}, 0, -1 \right), & S_{16} &= \frac{1}{2\sqrt{2}} \left(\sigma^2, -\frac{1}{\sigma}, -\frac{1}{\sigma}, -\frac{1}{\sigma} \right), \\ S_{17} &= \frac{1}{2\sqrt{2}} \left(\sigma^2, \frac{1}{\sigma}, \frac{1}{\sigma}, -\frac{1}{\sigma} \right), & S_{18} &= \frac{1}{2\sqrt{2}} \left(\sigma^2, -1, -\frac{1}{\sigma^2}, 0 \right), \\ S_{19} &= \frac{1}{2\sqrt{2}} \left(\sigma^2, 1, -\frac{1}{\sigma^2}, 0 \right), & S_{20} &= \frac{1}{2\sqrt{2}} \left(\sigma^2, 0, -1, \frac{1}{\sigma^2} \right). \end{aligned}$$

(2) Images by the Clifford translation g_i of the face F_i of \mathcal{F} and of its edges.

g_1 maps F_1 to F_7 , and we have for the vertices and the edges:

$$\begin{aligned} g_1(S_3) &= S_6, & g_1(S_{18}) &= S_8, & g_1(S_{16}) &= S_{11}, & g_1(S_5) &= S_{17}, & g_1(S_{20}) &= S_2, \\ g_1(\widehat{S_3 S_{18}}) &= \widehat{S_6 S_8}, & g_1(\widehat{S_{18} S_{16}}) &= \widehat{S_8 S_{11}}, & g_1(\widehat{S_{16} S_5}) &= \widehat{S_{11} S_{17}}, & g_1(\widehat{S_5 S_{20}}) &= \widehat{S_{17} S_2}, \\ g_1(\widehat{S_{20} S_3}) &= \widehat{S_2 S_6}. \end{aligned}$$

g_2 maps F_2 to F_8 , and we have for the vertices and the edges:

$$\begin{aligned} g_2(S_{18}) &= S_{15}, & g_2(S_{12}) &= S_{17}, & g_2(S_9) &= S_2, & g_2(S_7) &= S_{19}, & g_2(S_3) &= S_4, \\ g_2(\widehat{S_{18} S_{12}}) &= \widehat{S_{15} S_{17}}, & g_2(\widehat{S_{17} S_2}) &= \widehat{S_8 S_{11}}, & g_2(\widehat{S_9 S_7}) &= \widehat{S_2 S_{19}}, & g_2(\widehat{S_7 S_3}) &= \widehat{S_{19} S_4}, \\ g_2(\widehat{S_3 S_{18}}) &= \widehat{S_4 S_{15}}. \end{aligned}$$

g_3 maps F_3 to F_9 , and we have for the vertices and the edges:

$$\begin{aligned} g_3(S_3) &= S_1, & g_3(S_7) &= S_{11}, & g_3(S_{10}) &= S_{17}, & g_3(S_{14}) &= S_{15}, & g_3(S_{20}) &= S_{13}, \\ g_3(\widehat{S_3 S_7}) &= \widehat{S_1 S_{11}}, & g_3(\widehat{S_7 S_{10}}) &= \widehat{S_{11} S_{17}}, & g_3(\widehat{S_{10} S_{14}}) &= \widehat{S_{17} S_{15}}, \\ g_3(\widehat{S_{14} S_{20}}) &= \widehat{S_{15} S_{13}}, & g_3(\widehat{S_{20} S_3}) &= \widehat{S_{13} S_1}. \end{aligned}$$

g_4 maps F_4 to F_{10} , and we have for the vertices and the edges:

$$\begin{aligned} g_4(S_{20}) &= S_9, & g_4(S_{14}) &= S_8, & g_4(S_{19}) &= S_{11}, & g_4(S_4) &= S_1, & g_4(S_5) &= S_{12}, \\ g_4(\widehat{S_{20} S_{14}}) &= \widehat{S_9 S_8}, & g_4(\widehat{S_{14} S_{19}}) &= \widehat{S_8 S_{11}}, & g_4(\widehat{S_{19} S_4}) &= \widehat{S_{11} S_1}, & g_4(\widehat{S_4 S_5}) &= \widehat{S_1 S_{12}}, \\ g_4(\widehat{S_5 S_{20}}) &= \widehat{S_{12} S_9}. \end{aligned}$$

g_5 maps F_5 to F_{11} , and we have for the vertices and the edges:

$$g_5(S_5) = S_{10}, \quad g_5(S_4) = S_6, \quad g_5(S_{15}) = S_8, \quad g_5(S_{13}) = S_9, \quad g_5(S_{16}) = S_7,$$

$$g_5(\widehat{S_5 S_4}) = \widehat{S_{10} S_6}, \quad g_5(\widehat{S_4 S_{15}}) = \widehat{S_6 S_8}, \quad g_5(\widehat{S_{15} S_{13}}) = \widehat{S_8 S_9}, \quad g_5(\widehat{S_{13} S_{16}}) = \widehat{S_9 S_7}, \\ g_5(\widehat{S_{16} S_5}) = \widehat{S_7 S_{10}}.$$

g_6 maps F_6 to F_{12} , and we have for the vertices and the edges:

$$g_6(S_{16}) = S_{19}, \quad g_6(S_{13}) = S_2, \quad g_6(S_1) = S_6, \quad g_6(S_{12}) = S_{10}, \quad g_6(S_{18}) = S_{14}, \\ g_6(\widehat{S_{16} S_{13}}) = \widehat{S_{19} S_2}, \quad g_6(\widehat{S_{13} S_1}) = \widehat{S_2 S_6}, \quad g_6(\widehat{S_1 S_{12}}) = \widehat{S_6 S_{10}}, \\ g_6(\widehat{S_{12} S_{18}}) = \widehat{S_{10} S_{14}}, \quad g_6(\widehat{S_{18} S_{16}}) = \widehat{S_{14} S_{19}}.$$

Then we define the equivalence classes on \mathcal{F} by:

$$q \in \mathring{\mathcal{F}} \Rightarrow \dot{q} = \{q\}, \\ \exists(i, j, k), q \in F_i \cap F_j \cap F_k \Rightarrow \dot{q} = \{q, g_i(q), g_j(q), g_k(q)\}, \\ (\exists(i, j), q \in F_i \cap F_j) \text{ and } (\forall k \neq i, j, q \notin F_k) \Rightarrow \dot{q} = \{q, g_i(q), g_j(q)\}, \\ (\exists i, q \in F_i) \text{ and } (\forall j \neq i, q \notin F_j) \Rightarrow \dot{q} = \{q, g_i(q)\}.$$

Here the integers i, j, k belong to $\{1, \dots, 12\}$, and F_i denotes a face of \mathcal{F} .

REFERENCES

- [1] R. AURICH, S. LUSTIG, F. STEINER. CMB anisotropy of the Poincaré dodecahedron. Class. Quantum Grav., 22: 2061-2083, 2005.
- [2] Al. BACHELOT. On the Klein-Gordon equation near a De Sitter brane in an Anti-de Sitter bulk. J. Math. Pures Appl., 105, 165-197, 2016.
- [3] Ag. BACHELOT-MOTET. Wave Computation on the Poincaré Dodecahedral Space. Class. Quantum Grav., 30-23:235010, 2013.
- [4] C. L. BENNETT, D. LARSON, J. L. WEILAND, N. JAROSIK, G. HINSHAW, N. ODEGARD, K. M. SMITH, R. S. HILL, B. GOLD, M. HALPERN, E. KOMATSU, M. R. NOLTA, L. PAGE, D. N. SPERGEL, E. WOLLACK, J. DUNKLEY, A. KOGUT, M. LIMON, S. S. MEYER, G. S. TUCKER, E. L. WRIGHT. Nine-Year Wilkinson Microwave Anisotropy Probe (WMAP) Observations: Final Maps and Results. ApJS, 208-2, 2013.
- [5] S. CAILLERIE, M. LACHIÈZE-REY, J.-P. LUMINET, R. LEHOUCQ, A. RIAZUELO, J. WEEKS. A new analysis of the Poincaré dodecahedral space model. Astron. Astrophys., 476-2: 691-696, 2007.
- [6] S. H. CHRISTIANSEN. Foundations of finite element methods for wave equation of Maxwell type. Springer, Applied Wave Mathematics, 335, 2009.
- [7] R. DAUTRAY, J.-P. LIONS, Mathematical Analysis and Numerical Methods for Science and Technology, Volume 5 Evolution Problems I. Springer-Verlag, 2000.
- [8] E. GAUSSMANN, R. LEHOUCQ, J.-P. LUMINET, J.-Ph. UZAN, J. WEEKS. Topological lensing in spherical spaces. Class. Quantum Grav., 18: 5155-5186, 2001.
- [9] W. EL. HANAFY, G. L. NASHED. Reconstruction of $f(T)$ -gravity in the absence of matter. doi="10.1007/s10509-016-2786-0", Astrophys. Space Sci., 2016.
- [10] A. IKEDA. On the spectrum of homogeneous spherical space forms. Kodai Math. J., 18: 57, 1995.
- [11] P. KEAST url:nines.cs.kuleuven.be Moderate-degree tetrahedral quadrature formulae Comput. Methods Appl. Mech. Engrg., 55, 1986, 339–348.
- [12] M. LACHIÈZE-REY. Eigenmodes of dodecahedral space. Class. Quantum Grav., 21:2455-2464, 2004.
- [13] R. LEHOUCQ, J. WEEKS, J.-Ph. UZAN, E. GAUSSMANN, J.-P. LUMINET. Eigenmodes of three-dimensional spherical spaces and their application to cosmology. Class. Quantum Grav., 19:4683-4708, 2002.
- [14] J. LERAY. Hyperbolic differential equations, Princeton University Press, 1953.
- [15] J.-P. LUMINET, B. F. ROUKEMA. Topology of the Universe: Theory and Observation, Theoretical and Observational Cosmology, 541, 117:156, 1999.
- [16] J.-P. LUMINET. The shape and topology of the universe. arXiv:0802.2236 [astro-ph], 2008.

- [17] J.-P. LUMINET, J. WEEKS, A. RIAZUELO, R. LEHOUCQ, J.-Ph. UZAN. Dodecahedral space topology as an explanation for weak wide-angle temperature correlations in the cosmic microwave background. Letters to nature, 425, 593:595, 2003.
- [18] B. MCINNES. APS Instability and the Topology of the Brane-World. arXiv: hep-th/0401035v4, 2004. Phys.Lett.B593:10-16,2004
- [19] F. W. J. OLVER, D. W. LOZIER, R. F. BOISVERT, and C. W. CLARK. url: NIST Digital Library of Mathematical Functions Print version: Cambridge University Press, New York, NY, 2010.
- [20] B. F. ROUKEMA, T. A. KAZIMIERCZAK. The size of the Universe according to the Poincaré dodecahedral space hypothesis. arXiv:1106.0727v2 [astro-ph.CO], 2011. Astronomy and Astrophysics 533 (2011) A11
- [21] P. SCOTT. The geometries of 3-manifolds. Bull. London. Math. Soc.,15:401-487, 1983.
- [22] H. TANABE. Equations of Evolution. Monographs and Studies in Mathematics, 6, 1979.
- [23] A.VASY. The wave equation on asymptotically de Sitter-like spaces. Adv. Math. 223 (2010), 49–97.
- [24] C. WEBER, H. SEIFERT. Die beiden Dodekaederräume. Math. Z., 37:237-253,1933.
- [25] J. WEEKS. Reconstructing the global topology of the universe from the cosmic microwave background. Class. Quantum Grav., 15: 2599-2604, 1998.
- [26] J. WEEKS. The Poincaré dodecahedral space and the mystery of the missing fluctuations. Notices of the AMS, 51-6: 610-619, 2004.
- [27] J. A. WOLF. Spaces of Constant Curvature. 5th edn (Boston, MA: Publish or Perish),1967.

UNIVERSITÉ DE BORDEAUX, INSTITUT DE MATHÉMATIQUES, UMR CNRS 5251, F-33405 TALENCE
CEDEX

E-mail address: `marie-agnes.bachelot@u-bordeaux.fr`, `alain.bachelot@u-bordeaux.fr`